96-55

Evaluation of High Resolution Seismic Reflection Surveying at Fort Bragg Army Post Fayetteville, North Carolina

by
Richard D. Miller
Jianghai Xia

technical support
Joe M. Anderson
David R. Laflen

manuscript preparation
Mary C. Brohammer
P. Acker

of the
Kansas Geological Survey
University of Kansas
Lawrence, Kansas

preliminary report submitted to
U.S. Geological Survey — WRD
North Carolina District
Raleigh, North Carolina

January 31, 1996

Kansas Geological Survey
Open-file Report

Disclaimer

The Kansas Geological Survey does not guarantee this document to be free from errors or inaccuracies and disclaims any responsibility or liability for interpretations based on data used in the production of this document or decisions based thereon. This report is intended to make results of research available at the earliest possible date, but is not intended to constitute final or formal publication.

SUMMARY

Shallow high resolution seismic techniques were evaluated at Fort Bragg Military Reservation near Fayetteville, North Carolina, to determine their resolution and detection potential for targets ranging in depth from the surface to over 100 ft of depth. The interval of interest was predominantly within the unconsolidated sands, clays, and gravels that lie above bedrock in this area. The study was concentrated within the Fort Bragg Containment Area (FBCA) which is divided into multiple Solid-Waste management Units (SWMUs). Individual sites within each of these SWMUs possess different types of potential environmental hazards including abandoned landfills, underground storage tanks, oil-water separators, vehicle repair and storage yards, as wells as many other unique land usages. The shallowest reflection event imaged with confidence during this test was about 50 ft deep, while the deepest was just over 250 ft. The near-surface hydrology is influenced at FBCA by repetitive interbedded sand (10-15 ft thick) and clay units (1-3 ft thick) of unknown horizontal extent. The finely-spaced lateral sampling and resolution of the shallow seismic reflection technique (as determined by this study) represents a relatively non-invasive tool that could assist in the assignment of hydrologic parameters and constraints necessary for effective modeling of transport and fate scenarios at many locations around the Fort.

Two different surface acoustic reflection methods were evaluated for resolution, signal-to-noise ratio, imagible depth range, and optimum equipment and parameters for effective imaging and correlation of acoustic features with existing geologic, hydrogeologic, and geophysical data. Multi-fold compressional and shear wave reflection surveying was evaluated by incorporating a series of walkaway noise tests with short CDP profiles near existing monitor wells. At both background test sites a compressional wave check shot velocity survey was acquired in a water-filled PVC cased monitor well several tens of feet from the survey lines. The compressional wave survey provided a subsurface image that could be interpreted with a much higher degree of confidence than the shear wave data. The shear wave data sets possessed a significantly higher resolution potential based on dominant wavelength alone, but due to the narrow band characteristics of the S-wave data, confident separation of individual reflection events and identification of the various converted modes was not possible. P-wave reflection surveying will provide hydrologic modelers with the most useful data for delineating stratigraphic and structural features of significance at the sites tested on Fort Bragg.

The two sites chosen for testing possessed unique near-surface conditions. Background site #1 (Figure 1A) was near an existing cluster of wells and within an area previously utilized by the Fort. Four different seismic sources, two different techniques, and two different types of receivers were evaluated during the walkaway portion of this study. After on-site evaluation of the test data, two P-wave CDP profiles and one S-wave CDP profile were acquired along two different test lines that intersected each other at about a 90 degree angle. A total of 190 shotpoints of 24-fold data were recorded at Background site #1. Background site #2 (Figure 1B) was along an access road leading to a remote field range near the western extreme of the study area. A well cluster was located near the southern end of the test line. Four different sources and two techniques were also evaluated at site #2. Two CDP surveys acquired along a single test line recorded a total of about 25 shotpoints of 24-fold data. This series of tests provided the necessary background to estimate resolution potential, effective imaging depths, guidelines for parameter design, equipment requirements, and overall effectiveness of shallow seismic reflection for future surveys within the FBCA.

INTRODUCTION

Understanding and quantifying the various factors that control transport and fate of contaminates associated with the long history of military activity at Fort Bragg Army Post near Fayetteville, North Carolina, is critical to current groundwater management and future remediation efforts. Fort Bragg is an active military facility serving as a training and staging area for the 18th Airborne Corps, 82nd Airborne Division, Special Forces, and several other very specialized groups and associated support units. Most operations that might represent potential environmental hazards on the Fort are likely related to vehicle maintenance (i.e., motor pools), specialized emergency training facilities (i.e., burn pits), landfills, fuel storage (both commercial and military), and chemical treatment facilities (i.e., dry cleaners, paint shops, etc.). Development of a site characterization program formulated specifically for certain types of problems requires a thorough evaluation of specific techniques and tools so limitations and appropriate applications of each can be established.

This investigation into potential applications of shallow seismic reflection techniques was undertaken in association with a Fort-wide program to evaluate various geophysical techniques for application to existing and future problems. The

primary focus of this study was to determine what capabilities and limitations the technique possessed, based on the present state-of-the-art, in the unique geologic setting of Fort Bragg. Background test sites were selected after consideration of available ground truth (geologic control through borehole information), geological and hydrological similarities to areas with or potentially with contaminate problems elsewhere on the Fort, and physical requirements of the various geophysical techniques tested or to be tested. Shallow seismic reflection was tested at two sites each with relatively unique surface and near-surface characteristics.

Shallow high resolution seismic techniques possess the necessary resolution potential in the McPherson Creek and Litte River Valley alluvium to delineate bed separations of 6 ft at depths between 40 and 100 ft. Shallow P-wave reflection surveys have routinely been successful imaging a shallow bedrock surface (< 100 m) as well as overlying unconsolidated sequences (Miller et al., 1989; Pullan and Hunter, 1990; Miller et al., 1986; Birkelo et al., 1987; Jongerius and Helbig, 1988; Goforth and Hayward, 1992). With the resolution potential of shallow S-wave surveys in comparison to P-wave surveys it is important in some situations to evaluate the feasibility of S-wave surveys (Pullan et al., 1990; Hasbrouck, 1991). The consistent shortcoming of S-wave surveys has been the very limited bandwidth resulting in minimal wavelet separation, which in turn makes unique interpretations of reflecting events impossible. An uphole survey or velocity check shot survey can provide conclusive verification of seismic reflection interpretations.

At least one 24-fold CDP line was acquired at each site with both P-wave and S-wave techniques. Incorporating the event identification potential of walkaway testing and the redundancy of the CDP method (Mayne, 1962) provided an excellent basis for feasibility estimations and determination of resolution potential. The uphole surveys were acquired primarily to allow accurate time-to-depth conversion of reflections interpreted on the stacked sections, thereby enhancing correlation of reflections with drill identified geologic interfaces. The integration of the various acoustic methods with the borehole-derived geology greatly enhanced evaluation of the techniques.

Meaningful correlation of two-way travel time reflections on CDP stacked section with borehole-encountered geologic contacts and comparison of modeled hyperbolae with interpreted reflection curves requires an accurate average velocity that only a surface-to-borehole or borehole-to-surface acoustic survey can provide. Incorporation of uphole acoustic velocity surveys, borehole geophysical logs, and

lithologic logs with land seismic data should provide the most accurate and horizontally continuous representation of the unconsolidated lithology at this site.

This feasibility survey was completed in a single trip with visits to two different sites at FBCA between September 28th and 30th, 1994. The most extensive study was undertaken at background site #1 on the 28th and 29th and included the acquisition of a series of walkaway noise tests (26 P-wave and 18 S-wave shot gathers), an uphole survey (sampling on 5 ft intervals between 30 and 80 ft of depth), two intersecting P-wave CDP profiles (119 shotpoints with sledgehammer/plate and a 53 shotpoint downhole 30.06 line), and a 15 shotpoint S-wave CDP profile (Figure 1A). Occupation of background site #2 was on the 30th and included a group of walkaway noise tests (32 P-wave and 8 S-wave shot gathers), two uphole surveys (19 records acquired at 6 different intervals between 30 and 90 ft), a P-wave CDP profile that included 24 stations, and a S-wave CDP survey over 10 stations (Figure 1B). This extensive series of tests provided sufficient background information to allow the design and execution of seismic reflection surveys optimized for near-surface conditions and survey objectives.

DATA ACQUISITION

Several different types of acoustic surveying methods or techniques were employed to determine the feasibility and specifications of future surveys to accurately image geologic contacts/interfaces between 30 and 100 ft deep. All data for this study were acquired on a Geometrics 2401X, 48-channel seismograph in SEG2 format. This seismograph amplifies, filters (analog), digitizes the analog signal into a 15-bit word, and stores the digital information in a demultiplexed format. Analog filters have an 18 dB/octave roll-off from the selected -3 dB points. A 1/5 msec sampling interval resulted in a 200 msec record with a 2500 Hz Nyquist frequency. A variety of analog low-cut filters were selected to allow determination of the optimum analog filter necessary to maximize the instantaneous dynamic range of the seismograph. Analog low-cut filters are necessary to properly shape the spectrum, allowing the maximum resolution possible for signal generated at this site (Steeples, 1990).

The very site-dependent nature of compressional wave source characteristics (Miller et al., 1994) prompted comparison of three types of sources, including the 30.06 downhole rifle (projectile), the 12-gauge auger gun (downhole explosive), and a 5.5 kg sledge hammer (weight drop). Each of these sources was used during the

walkaway testing and, due to favorable characteristics, the downhole 30.06 and sledgehammer were used during the acquisition of P-wave CDP data. The very shallow depth to the bedrock reflector and thin beds that overlay bedrock made it imperative that a broadband high frequency source wavelet be produced and propagated. The sources selected for testing comprise a good cross-section of low-energy impulsive compressional wave sources.

From wave theory it is easy to see that S-wave velocities could be as much as 1/4 and maybe even 1/10 the velocity of P-waves for a given earth layer (Pullan et al., 1990). Assuming the spectral characteristics do not significantly decrease, this lower S-wave velocity, in comparison to a P-wave velocities at the same site, increases the resolution potential of S-wave data. This increase in resolution can only be actualized if the reflection frequency bandwidth and upper corner frequency does not decrease more than the velocity. The source is key to maintaining a broad bandwidth and relatively high corner frequency. For this test the MiniBlock (sledge horizontal impact on a steel plated wood post) was used to generate translational waves. The lack of an extensive shear wave source test was justified by the very minimal differences and unique nature of most S-wave sources (Miller et al., 1992).

Receivers for this study included single Mark Products L-40A 100 Hz vertical geophones, Mark Products L-40A 50 Hz horizontal geophones, and a Mark Products P-44 10 Hz hydrophone. The target interval and resolution requirements dictated the use of high natural frequency geophones with optimum coupling and close spacing. Available for testing if the 100 Hz vertical geophones could not produce an acceptable output were triple Mark Products L-28E 40 Hz geophones wired in series. The hydrophone requires at least 10 ft of water column to produce a linear response to acoustic energy in the borehole. High quality receivers are essential for cleanly recording the high frequency, low amplitude signal characteristic of shallow seismic surveys.

Ground truth is essential for the correlation of interpreted reflection hyperbolae to reflectors in the subsurface. Reflection events identified on shot gathers can only be confidently verified through modeling hyperbolae with borehole-measured average velocity. The most reliable way to match time measured on a seismogram with depth is through an uphole survey (check shot survey, downhole survey. etc.). As a part of this study, uphole surveys were acquired at both sites using a downhole hydrophone and multiple stacked impacts of a sledge hammer on a steel plate. The

resulting time-to-depth conversions allow accurate correlation of reflection to reflector.

Quality assurance/quality control (QA/QC) were critical and continuous throughout acquisition and processing. Near-surface inconsistencies, traffic noise, jet aircraft noise, the extremely narrow and changing optimum recording window, and high moisture conditions made establishing QA/QC guidelines and meticulous monitoring of data an absolutely essential aspect of the data acquisition. Based on subtle changes in the near-surface, minor adjustments to some parameters (e.g., source to near offset) were necessary to maintain the optimum recording window (Hunter et al., 1984). The seismograph CRT display, nearly real-time digital filtering, and real-time graphical display of noise levels permitted instantaneous monitoring of not only cultural, air traffic, and vehicle traffic noise, but also cable-to-ground leakage and geophone plant quality. After each geophone was planted it was tested to insure a cable-to-ground resistance greater than 1000K ohms and an individual geophone continuity of 500 ohms (±20 ohms). As well, each geophone underwent a modified tap and twist test. No shot was recorded if background noise voltage levels on active geophones was greater than 0.05 mV. The ability of the seismograph to real-time monitor noise levels, signal quality (through digital filtering), and unacceptable geophone plants, and the roll-switch's built-in earth leakage and continuity meters minimized the chances that any recorded shot would not be maximized for the site and equipment.

DATA PROCESSING

Data from this study were processed on an Intel P-class microcomputer using *Eavesdropper* and *WinSeis*, both commercially available algorithms. Display parameters were determined based on scale of existing data sets, optimum exaggerations, and workable formats. During this study, the only operations or processes used were those that enhanced the signal-to-noise ratio and/or resolution potential as determined through evaluation of high confidence reflections identified on field files.

The principal utility of a walkaway noise test is to expedite and improve equivalent comparisons of various source, receiver, and instrument settings and configurations as they relate to overall improvements in the signal-to-noise ratio and frequency content. Walkaway tests are ideally suited to the identification of individual events within the full wave field. Phase velocity and wave types are

probably the most important pieces of information extractable from walkaways. Their importance is related to the dependence of velocity and wave type on spread geometries and offsets (Pullan and Hunter, 1985). The level of testing is dependent on the objectives of the project and degree of difficulty obtaining the required resolution. Processing of walkaway data for this study was limited to trace organizing, gain balancing, and digital filtering. Walkaway data from each source configuration or comparison parameter are displayed in a source-to-receiver order.

For most basic shallow high-resolution seismic reflection data, CDP processing steps are a simple scaling down of established petroleum-based processing techniques and methods (Yilmaz, 1987; Steeples and Miller, 1990). The processing flow for the CDP stacked sections was similar to that used for routine petroleum exploration (Table 1). The main distinctions relate to the conservative use and application of correlation statics, precision required during velocity and spectral analysis, and the accuracy of the muting operations. A very low (by conventional standards) allowable NMO stretch (< 20%) was extremely critical in minimizing contributions from the very shallow reflected energy at offsets significantly beyond the critical angle. Limiting wavelet stretch through muting maximizes resolution potential and minimizes distortion in the stacked wavelets (Miller, 1992). Even with an awareness of problems resulting from stretch and the interference of refractions with reflection, artifacts of remnant refractions and sample stretch can be observed in stacked data from both sites. Variability in depth of the first refracting horizon was as much as 10 msec across a single CDP stacked section, suggesting sufficient changes in depth to bedrock to require compensation. Operations such as refraction statics will be required to effectively compensate for this depth variability. Processing/processes used on this data have been carefully executed with no *a priori* assumptions. Extreme care was taken to enhance through processing only what could be identified on raw data and not to create coherency on stacked sections.

Most processing steps/operations applied to shallow high-resolution seismic reflection data sets during the generation of CDP stacked sections are a simple scaled-down version of established processes developed for exploration of petroleum interests. Some processes have assumptions that are simply violated by most shallow reflection data sets and application of these processes could dramatically reduce data quality or worse, generate artifacts. In particular, in processes such as deconvolution and some forms of trim statics there is an assumption of a large number of reflections with a random reflectivity sequence and high signal-to-noise

ratios (Yilmaz, 1987). Migration is another process that, due to non-conventional scaling, many times appears to be necessary when geometric distortion may be simple scale exaggeration. With extremely low near-surface velocities corrections are extremely minimal (Black et al., 1994). The low-pass nature and coherency enhancing tendency of fk migration improves geometric accuracy but reduces resolution potential of reflections on CDP stacked sections. Consistency in arrival and apparent orientation of individual reflections after each process was critical to insuring the authenticity of final interpretations.

RESULTS

Shallow seismic reflection is a method that lends itself to over-processing, inappropriate processing, and minimal involvement processing. Interpretations must take into consideration not only the geologic information available but also each step of the processing flow and the presence of reflection events on raw unprocessed data. Identification and confirmation of reflection hyperbolae on walkaway noise tests is essential and best accomplished through mathematical curve fitting, incorporating borehole-derived velocity structure and comparison of file-to-file consistency. Walkaway noise tests should be designed so the subsurface is significantly over-sampled horizontally and the source-to-farthest receiver offset is about twice the depth of interest. This allows for all aspects of the complete wave field (especially the reflections) to be thoroughly appraised. Walkaway tests performed at background site #1 and background site #2 were in close proximity to well clusters which are essential as control points for correlation between observed hyperbolic curves and actual vertically measured average velocity.

Background Site #1

The receivers for the P-wave and S-wave experiment at site #1 were laid along a north/south line with 2 ft and 4 ft intervals, respectively (Figure 1A). High signal-to-noise reflection events interpretable on P-wave sections possess a vertically incident time of about 35 to 45 msec (Figure 2). Modeling the shape of these proposed reflections with theoretical hyperbolic curves produces reasonable fit with reflectors at depths of about 80 to 100 ft and an NMO velocity of around 4000 ft/sec. From velocity check shots at site #1 the average velocity to 80 ft was just over 4000 ft/sec. It is therefore reasonable to be cautiously optimistic that this apparent curved arrival is a primary reflection.

Of the three sources tested at site #1, the downhole 30.06 possesses the highest signal-to-noise and resolution potential (Figure 3). The 200 Hz analog low-cut filter applied to all the sources dramatically reduces the ground roll and the 100 Hz refraction "ring." The sledge hammer provided equivalent or maybe slightly better signal-to-noise ratio, but less resolution potential, when compared to the downhole 30.06 when both are recorded with a 200 Hz analog low-cut filter (Figure 2). The strongest negative characteristics of the sledge hammer were the ratio of air-coupled wave to reflection energy, the potential for shot-to-shot inconsistent source energy, surface coupling, lower dominant frequency, and the slight degradation of resolution potential due to stacking. The auger gun data possessed an easily interpretable 40 msec reflection when recorded with a 200 Hz analog filter, but was a little too energetic and possessed a slightly lower reflection frequency bandwidth, which was likely as a direct result of the higher level of energy release (Knapp and Steeples, 1986) (Figure 4).

Digital filtering of shot gathers recorded with 200 Hz analog low-cut filters increased the upper corner frequency of the reflection bandwidth and resulted in a higher dominant frequency. The minimum phase characteristics of the downhole 30.06 became much more evident in comparison to either the sledge hammer or auger gun with data recorded with the 200 Hz analog filter. Analog filtering seems to provide a slightly broader bandwidth and higher resolution potential than nearly equivalent digital filtering. This pre-A/D spectral shaping allows the full dynamic range of the 15-bit seismograph to be exploited (Steeples, 1990). Analysis of compressional wave tests at site #1 leads to the following recommendations for P-wave CDP surveys at settings similar to site #1: the downhole 30.06 fired into shallow holes, recorded with 200 Hz analog low-cut filters, with 100 Hz geophones, a source and receiver spacing of 2 to 4 ft, and at least 24-fold redundant recording. Due to the unique nature of the 30.06 downhole seismic source, data acquired with a sledge hammer and plate would only slightly decrease the overall potential and therefore effectiveness of a reflection survey.

S-wave reflection testing provided encouraging results, considering the narrow bandwidth problems that chronically plague attempts to image unconsolidated sediments. A potential reflection event can be interpreted with a vertical incident time of around 240 msec and an apparent NMO velocity of around 1300 ft/sec (Figure 5). This reflection correlates to a reflector at a depth of about 90 ft. Occasionally on shot gathers collected for the S-wave CDP test line the same event

can be identified through noise at times consistent with the walkaway-interpreted event (Figure 6). Extreme care needs to be taken before placing confidence in identification of the apparent curved arrival between the refraction and ground roll as potential reflection events (Figure 6). Mode conversions and refraction ring resulting from narrow bandwidth are both possible explanation for many arrivals within that interval. With the lack of file-to-file consistency, most of these events are not good candidates for high confidence reflections. Based on observations of S-wave energy generated and recorded at background site #1, S-wave profiling does have potential, but the lack of file-to-file consistency and only a single high-confidence reflection event provides no advantages over compressional wave surveys to image acoustic interfaces within the unconsolidated material at this site.

Short CDP profiles using S- and P-wave energy were recorded at background site #1. Two P-wave profiles were recorded which intersected at nearly 90 degrees near the north end of study area (Figure 1A). Both P-wave CDP surveys were acquired using parameters and equipment determined to be optimum during the walkaway noise testing. The north/south line was coincident with the walkaway spread and provided a much higher signal-to-noise ratio image of the subsurface than the east/west profile (Figures 7 and 8). Besides the several hundred foot separation in the profile lines, the only difference between the two data sets is the redundancy or fold of the stacked data. The north/south line was acquired so a nominal 24-fold section could be produced while the east/west profile could at best produce a nominal 12-fold CDP stacked section. The improvement in data quality and therefore applicability to a wide range of problems is significantly greater with the higher fold data.

The CDP stacked S-wave data provides little in the way of interpretable reflections (Figure 9). The lack of stacked reflections is likely related to the file-to-file inconsistencies in apparent reflected arrivals noted previously during discussion of the walkaway noise tests. It is possible, with a longer line and polarity reversal/ stacking, that the events previously identified on shot gathers may become more pronounced. High amplitude linear arrivals have sufficiently saturated the stacked traces that little in the way of horizontally coherent potential reflection events can be interpreted.

Interpretations of stacked data from site #1 need to incorporate uphole data acquired in borehole #B7. The 23 ft water table limited the shallowest hydrophone reading to a depth of 30 ft. The average velocity from 30 ft to the ground surface was

approximately 2700 ft/sec, while the average velocity to 80 ft was calculated to be about 4100 ft/sec. This velocity structure would suggest a reflection from 80 ft should arrive at about 40 to 45 msec on P-wave CDP stacked sections.

Several reflection events stack coherently on the processed P-wave profile (Figure 7). Without a detailed geologic log, correlating reflections with reflectors is not possible for this report. Consistent with the field files, reflection arrivals are evident between about 30 and 80 msec. Events between 30 and 40 msec should be imagible and stack coherently on CDP sections. More data and greater attention to detail would likely result in reflections from depths as shallow as 75 ft at this site. The shallowest confidently interpretable event, arriving at about 35 to 40 msec, appears to have a slightly lower frequency than events later in time. Based on the knowledge that the earth attenuates high frequency, and therefore the dominant reflection frequencies should decrease with depth, the origin of this event becomes questionable. However, with the very good correlation between the CDP stack and field files of this reflection's stacking velocity, some confidence can be placed in its authenticity. Explanations for apparent reduced frequency include NMO stretch, incomplete removal of all the refraction wavelet, and elevated amplitudes from automatic gaining. Considering the likely geology at this site and reflection characteristics of the stacked data, the 40 msec event is likely bedrock with events deeper in the section being from within the consolidated rock sequence.

Background Site #2

Background site #2 was occupied to provide diversity and to insure some area-wide consistency in test data used to make general assessments of the applicability of shallow seismic reflection (Figure 1B). The slower average velocity in the upper 100 ft at this site translated into a much more conducive site for the recording of reflections from depths as shallow as 30 to 40 ft. The thicker near-surface layer is evident on walkaway shot gathers acquired when the source was off the north end of the line (Figure 10), as compared to when the source was south of the spread (Figure 11). The walkaway data at this site were recorded in a wooded area along a dirt path several hundred feet off a paved highway. The P-wave and S-wave CDP profiles were recorded along this same path. A strong coherent reflection event is evident to varying degrees on all P-wave walkaway shots recorded at this site. The dominant reflection frequency without analog low cut filtering on 30.06 data is about 125 Hz (Figure 12). Data acquired with a 200 Hz analog filter possesses a

dominant frequency of about 180 Hz and very good separation between the refraction and shallow reflecting events. The analog filtering clearly acts to balance the spectra, providing a relatively broad bandwidth and high upper corner frequency. The character of the 50 msec reflection is suggestive of a bedrock reflection when comparison is made with apparent events above and below this prominent event.

After comparison of the three compressional wave sources used for this study it is clear that here at site #2, as with site #1, the 30.06 downhole provides the best resolution potential; however, the sledge and plate represents a readily available substitute that would not result in a significant drop in data quality. The calculated NMO velocity from curve fitting on the shot gathers for the 45 msec reflection is about 4200 ft/sec and the depth is about 95 ft. This is consistent with the uphole survey which suggested an average velocity of about 4500 ft/sec from a depth of 90 ft. Some hints of shallower events are interpretable on the shot gathers. The shallowest of these events would have a vertical incident time of around 35 msec, which would equate to a depth of around 50 ft. The auger gun at this site generated a high percentage of low frequencies, but digital filtering sufficiently reduced the amplitude of these lower frequencies to yield a frequency band consistent with the 30.06 (Figure 13). The higher percentage of lower frequency energy manifests itself in a higher ground roll wave packet. Compressional wave data from this site possesses greater potential to image reflectors between the bedrock surface and about 30 or 40 ft of depth than that from the first background site.

The CDP stacked section acquired at this site does not contain cleanly separated reflection events. This ringy appearance is due to bandwidth problems and the minimal number of shot gathers incorporated into the stack (Figure 14). The shallowest event that stacks coherently is at about 45 msec and is likely a combination of shallow reflection and refraction. From shot gathers it is clear that a strong reflection should be present on stacked section at about 45 to 50 msec. The presence of the strong 45 msec reflection on shot gathers and observations made during each step of the processing flow are the basis for suggesting reflection and refraction energy combined to produce the event present at 45 msec on the CDP stacked section. Deeper reflection events do not possess sufficient optimum offset traces to provide a meaningful acoustic picture of the subsurface below bedrock. Increasing the number of shots would allow better editing and statistical evaluations and, therefore, CDP stacked sections from this site should improve to be as good and probably better than site #1.

Shear wave walkaway tests at site #2 did not result in as optimistic a projection as to the effectiveness of S-waves in improving resolution of equivalent P-wave surveys. There is, however, strong evidence to support the suggestion that at least one reflected S-wave arrival was recorded at site #2. A possible reflection arrival can be observed with a zero offset time of around 230 msec on several shot gathers (Figure 15). This arrival is time- and apparent velocity-consistent with events observed at site #1. The main distinction between the two sites is the significant decrease in signal-to-noise ratio at site #2. The bandwidth is narrow, as at site #1, limiting the effectiveness of S-waves since distinguishing unique arrivals becomes virtually impossible when the bandwidth is too narrow. The lack of good confidence in identifying reflection arrivals on field files negated the necessity of CDP stacking shot gathers collected for that purpose.

Uphole surveys at this site were acquired in borehole #BS2-W1. Data were taken on the west side of the borehole while lowering the hydrophone and on the east side of the borehole while raising the hydrophone. The two surveys were extremely consistent, providing valuable average velocity information for equating interpreted reflections with depth. The uphole survey also allowed modeled reflection curves derived from shot gathers to be verified with the true average velocity. Based on initial analysis it appeared the average velocities as determined from reflection curvature might be slightly less than at site #1 but, after examination of the reversed refraction information, the stacking velocity is not only consistent with site #1, it is also very close to the true average as determined through borehole measurements. It is very evident from refraction analysis the thickness of near-surface material increases to the north. The variability in the near surface is significant and CDP processing flows should incorporate techniques to compensate for these changes.

CONCLUSIONS

The walkaway testing, check shot surveys, and CDP profiles were designed and executed to evaluate the acoustic signature, optimum acquisition equipment and parameters, near-surface velocity structure, horizontal consistency in reflector character, generalized resolution potential and signal-to-noise ratio, and impact of cultural noise (i.e., air traffic, vehicle traffic, troop activities, etc.). The walkaway noise tests allowed definitive selection of equipment and parameters as well as optimum station spacing and resolution potential. The check shot surveys (uphole

velocity/one-way travel time) established an approximate velocity structure for the upper 80 ft of sediments in well #B7 at background site #1 (in the meadow) and well #BS2-W1 at background site #2 (in the woods). The check shot surveys were critical to correlating average velocity with curve-derived NMO velocities. The uphole surveys also allowed for future correlation of drill/log defined geology with reflections interpreted on CDP stacked sections. The compressional wave CDP profiles collected at the two sites suggest a practical vertical bed resolution on the order of 10 ft with a theoretical limit of around 6 ft. The majority of the reflections interpretable on the CDP stacked sections are from interfaces below the bedrock (suggested to be around 100 ft below ground surface).

Shallow seismic reflection techniques can be effective imaging the shallow subsurface at Fort Bragg Army Post. The shallowest depth that can be optimally imaged with seismic reflection would be about 40 to 50 ft. Based on the velocity structure of the unconsolidated sediments in the areas tested, it will be very difficult and likely impossible to practically image interfaces shallower than about 40 ft in this area with existing shallow seismic techniques. Shallower depths are possible but only with significant expense and extreme care. The bedrock surface should represent a target that can be easily imaged in most areas, with the maximum imagible depths limited by energy and source-to-receiver offsets. Compressional wave surveys will probably result in the most useful data in terms of signal-to-noise and wavelet characteristics, but if the bandwidth of the S-wave data could be increased even slightly, there are strong indications that higher resolution potential may result from S-wave surveys. Extreme care is necessary when processing data that target reflectors between bedrock and about 40 ft due to the subtle difference in the refraction and reflection curvature at longer offsets and the similar spectral characteristics of these two body wave arrivals. Acquisition of surface-to-borehole velocity profiles should be incorporated into all seismic surveys at Fort Bragg.

Considering the promise of shallow seismic reflection at Fort Bragg, it should be considered one of the geophysical tools available for subsurface characterization at sites where the continuity of unconsolidated layers between 40 ft and bedrock needs to be known, the surface topography of bedrock is important, delineation of structural features (faults, fractures, folding, dip angle, etc.) below the surface of bedrock is required, and/or delineation of the relative geometry of subsurface layers deeper than about 40 ft are necessary as part of hydrologic or geologic models.

ACKNOWLEDGMENTS

This work was supported by the U.S. Geological Survey under Contract #1434HQ-95-SA-0182. We appreciate the support and assistance of Alex P. Cardinell and Beth Wrege of the U.S. Geological Survey during acquisition and project preparation.

Table 1
Processing flow

Primary Processing

format from SEG2 to KGSEGY
preliminary editing (automatic bad trace edit with 10 msec noise window)
trace balancing (50 msec window)
first arrival muting (direct wave and refraction)
surgical muting (removal of ground roll based on trace-by-trace arrival)
assign geometries (input source and receiver locations)
sort into CDPs (re-order traces in common midpoints)
velocity analysis (whole data set analysis on 100 ft/sec increments)
spectral analysis (frequency vs amplitude plots)
NMO correction (station dependent ranging from 1200 [S-wave] to 4500 [P-wave] ft/sec)
correlation statics (2 msec max shift, 7 pilot traces, 100 msec window)
digital filtering (bandpass 75-150 500-750)
secondary editing (manual review and removal of bad or noisy traces)
CDP stack
AGC scale (100 msec window)
display

REFERENCES

Birkelo, B.A., D.W. Steeples, R.D. Miller, and M.A. Sophocleous, 1987, Seismic reflection study of a shallow aquifer during a pumping test: *Ground Water*, v. 25, p. 703-709.

Black, R.A., D.W. Steeples, and R.D. Miller, 1994, Migration of shallow seismic reflection data: *Geophysics*, v. 59, p. 402-410.

Goforth, T., and C. Hayward, 1992, Seismic reflection investigations of a bedrock surface buried under alluvium: *Geophysics*, v. 57, p. 1217-1227.

Hasbrouck, W.P., 1991, Four shallow-depth, shear-wave feasibility studies: *Geophysics*, v. 56, p. 1875-1885.

Hunter, J.A., S.E. Pullan, R.A. Burns, R.M. Gagne, and R.S. Good, 1984, Shallow seismic-reflection mapping of the overburden-bedrock interface with the engineering seismograph – Some simple techniques: *Geophysics*, v. 9, p. 1381-1385.

Jongerius, P., and K. Helbig, 1988, Onshore high-resolution seismic profiling applied to sedimentology: *Geophysics*, v. 53, p. 1276-1283.

Knapp, R.W., and D.W. Steeples, 1986, High-resolution common depth point seismic reflection profiling: field acquisition parameter design: *Geophysics*, v. 51, p. 283-294.

Mayne, W.H., 1962, Horizontal data stacking techniques: Supplement to *Geophysics*, v. 27, p. 927-938.

Miller, R.D., 1992, Normal moveout stretch mute on shallow-reflection data: *Geophysics*, v. 57, p. 1502-1507.

Miller, R.D., S.E. Pullan, D.A. Keiswetter, D.W. Steeples, and J.A. Hunter, 1992, Field comparison of shallow S-wave seismic sources near Houston, Texas: Kansas Geological Survey Open-file Report 92-33.

Miller, R.D., S.E. Pullan, J.S. Waldner, and F.P. Haeni, 1986, Field comparison of shallow seismic sources: *Geophysics*, v. 51, p. 2067-2092.

Miller, R.D. S.E. Pullan, D.W. Steeples, and, J.A. Hunter, 1994, Field comparison of shallow P-Wave seismic sources near Houston, Texas: *Geophysics*, v. 59, p. 1713-1728.

Miller, R.D., D.W. Steeples, and M. Brannan, 1989, Mapping a bedrock surface under dry alluvium with shallow seismic reflections: *Geophysics*, v. 54, p. 1528-1534.

Pullan, S.E., and J.A. Hunter, 1990, Delineation of buried bedrock valleys using the optimum offset shallow seismic reflection technique: Soc. Explor. Geophys. Investigations in Geophysics, Investigations in Geophysics no. 5, Stan H. Ward, ed., *Volume 3: Geotechnical*, p. 75-87.

Pullan, S.E., and J.A. Hunter, 1985, Seismic model studies of the overburden-bedrock reflection: *Geophysics*, v. 50, p. 1684-1688.

Pullan, S.E., J.A. Hunter, and K.G. Neave, 1990, Shallow shear-wave reflection tests [Exp. Abs.]: Soc. Expl. Geophys., p. 380-382.

Steeples, D.W., 1990, Early spectral shaping boosts data quality: *Oil and Gas Journal*, v. 88, no. 38, Sept. 17, p. 49-55.

Steeples, D.W., and R.D. Miller, 1990, Seismic-reflection methods applied to engineering, environmental, and groundwater problems: Soc. Explor. Geophys. Investigations in Geophysics, Investigations in Geophysics no. 5, Stan H. Ward, ed., *Volume 1: Review and Tutorial*, p. 1-30.

Yilmaz, O., 1987, Seismic data processing: Soc. Explor. Geophys. Investigations in Geophysics, Investigations in Geophysics no. 2, S.M. Doherty, ed., p. 1-30.

Figure Captions

Figure 1A Site map indicating approximate orientation of the seismic test area at both background site #1.

Figure 1B Site map indicating approximate orientation of the seismic test area at both background site #2.

Figure 2 Shot gather using the 5.5 kg sledge hammer and plate recorded with analog low-cut filters (a) out, (b) 50 Hz, (c) 100 Hz, and (d) 200 Hz. The source-to-receiver offsets ranged from 2 ft to 192 ft.

Figure 3 Shot gather using the downhole 30.06 projectile source recorded with analog low-cut filters (a) out, (b) 50 Hz, (c) 100 Hz, and (d) 200 Hz. The source-to-receiver offsets ranged from 2 ft to 192 ft.

Figure 4 Shot gather using the 12-gauge auger gun recorded with analog low-cut filters (a) out, (b) 50 Hz, (c) 100 Hz, and (d) 200 Hz. The source-to-receiver offsets ranged from 2 ft to 192 ft.

Figure 5 SH-wave recorded using the MiniBlock and 5.5 kg sledgehammer. An apparent reflection can be interpreted at about 250 msec.

Figure 6 A series of S-wave records recorded for summation into a CDP stacked section. The 250 msec reflection is evident on some records as well as a questionable reflection between the refraction and ground roll.

Figure 7 CDP stacked section #1 which was recorded from south to north starting near the well clusters. Several relatively strong reflections can be interpreted. It is possible that a portion of the shallowest high amplitude event could be a stacked combination of reflection and refraction.

Figure 8 CDP stacked section #2 which was recorded from west to east starting near the northern extreme of the well cluster. This section is extremely similar to Figure 7 with the exception of the decrease in signal to noise.

Figure 9 CDP stacked section of the S-wave data set. Little in the way of confidently identifiable reflection are present on this section. Lack of file-to-file consistency and a statistically small data set are at least in part responsible.

Figure 10 Shot gather using the 5.5 kg sledge hammer and plate recorded with analog low-cut filters (a) out, (b) 50 Hz, (c) 100 Hz, and (d) 200 Hz. The source-to-receiver offsets ranged from 2 ft to 192 ft.

Figure 11 Shot gather using the 5.5 kg sledge hammer and plate recorded with analog low-cut filters (a) out, (b) 50 Hz, (c) 100 Hz, and (d) 200 Hz. The source-to-receiver offsets ranged from 2 ft to 192 ft. This set of records is different from Figure 10 in the location of the shot relative to the receivers. The source was on the north end of the line with the receiver spread on the south.

Figure 12 Shot gather using the downhole 30.06 projectile source recorded with analog low-cut filters (a) out, (b) 50 Hz, (c) 100 Hz, and (d) 200 Hz. The source-to-receiver offsets ranged from 2 ft to 192 ft.

Figure 13 Shot gather using the 12-gauge auger gun recorded with analog low-cut filters (a) out, (b) 50 Hz, (c) 100 Hz, and (d) 200 Hz. The source-to-receiver offsets ranged from 2 ft to 192 ft.

Figure 14 CDP stacked section of compressional wave data. The very ringy appearance of the stacked data is likely related to the very small number of traces used to generate this section and the narrow band nature of the sledge hammer on stacked data.

Figure 15 SH-wave shot gathers which were acquired to be incorporated into a CDP stacked section, but without a more confidently interpretable reflection arrival a stacked section would not be terribly significant.

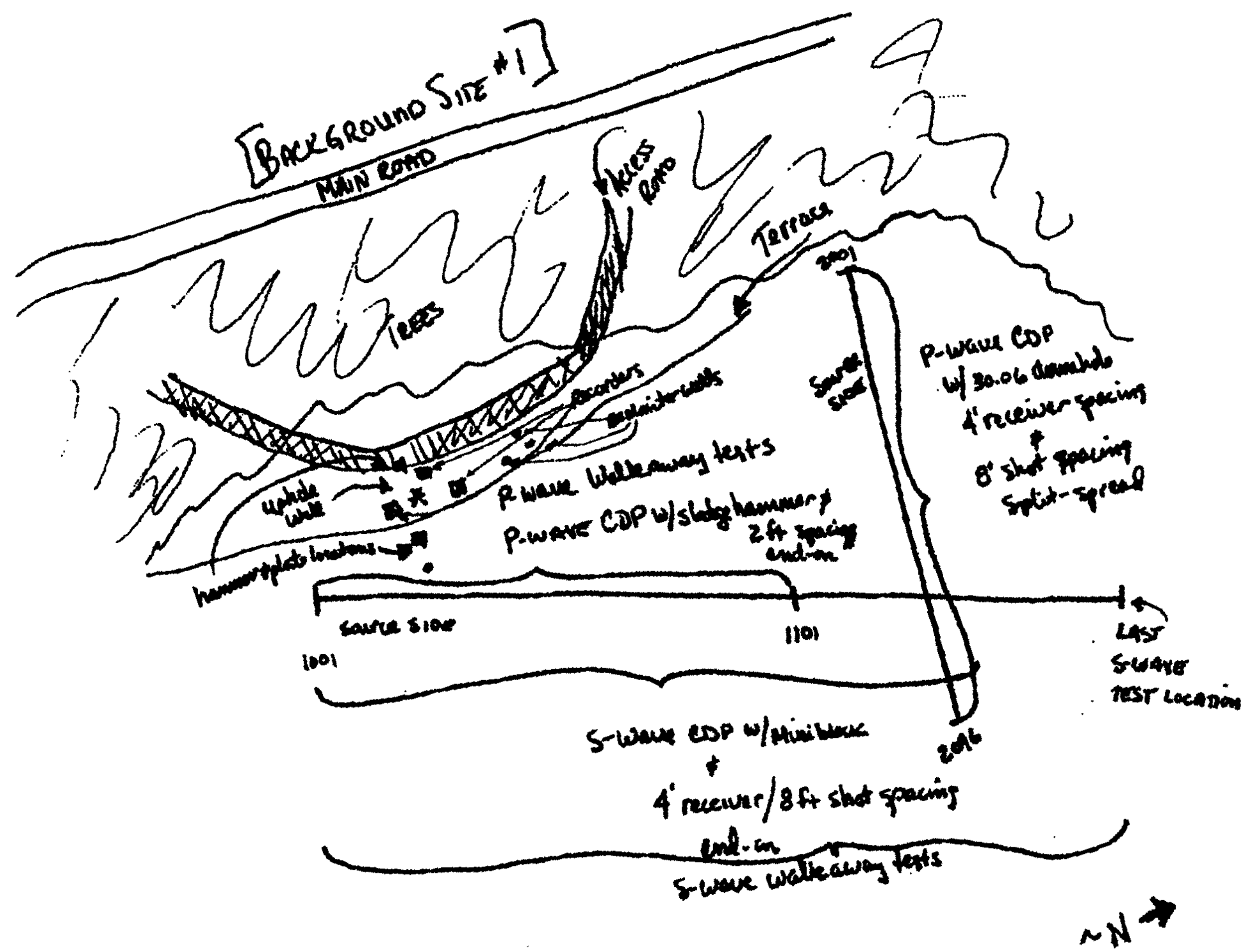
[BACKGROUND SITE #1]
MAIN ROAD
ACCESS ROAD
TREES
TERRACE
P-WAVE WALKAWAY TESTS
P-WAVE CDP W/ SLEDGE HAMMER & 2 FT SPACING END-ON
P-WAVE CDP W/ 30.06 DOWNHOLE 4' RECEIVER SPACING & 8' SHOT SPACING SPLIT-SPREAD
SOURCE SIDE
1001
1101
2001
2096
LAST S-WAVE TEST LOCATION
S-WAVE CDP W/ MINIBANG & 4' RECEIVER/8 FT SHOT SPACING END-ON
S-WAVE WALKAWAY TESTS
~N

Figure 1A

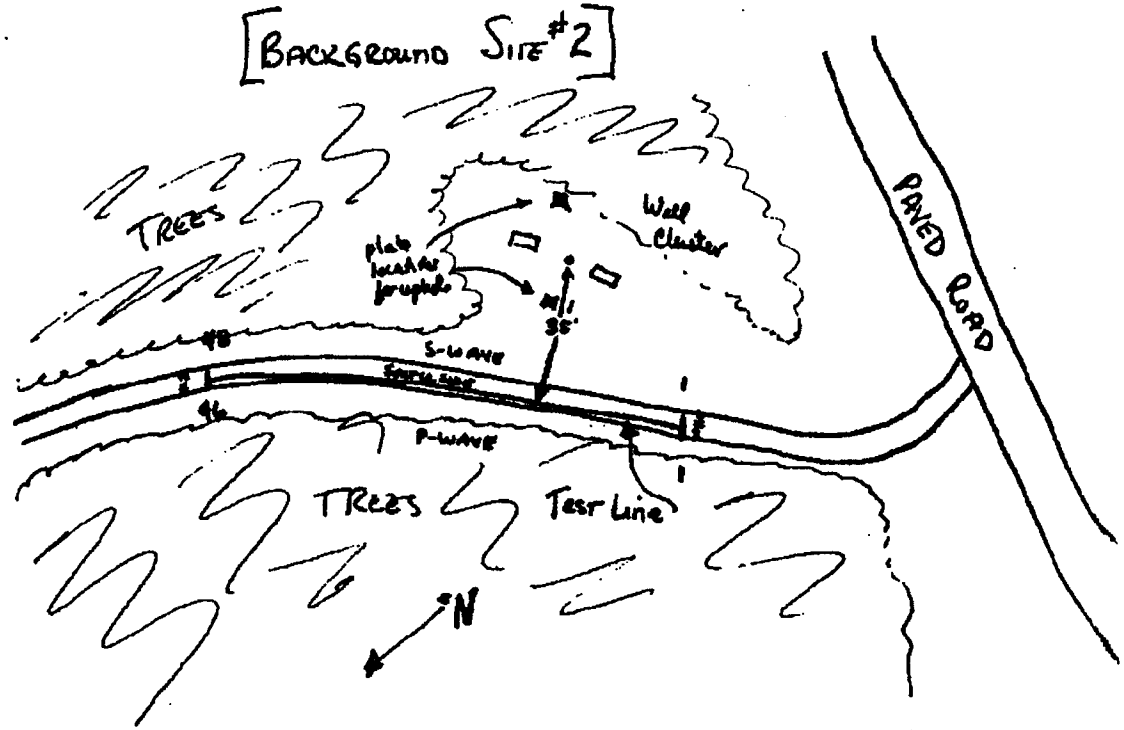
[Background Site #2]
TREES
Well Cluster
PAVED ROAD
S-WAVE
P-WAVE
TREES
Test Line
N

Figure 1B

Figure 2a

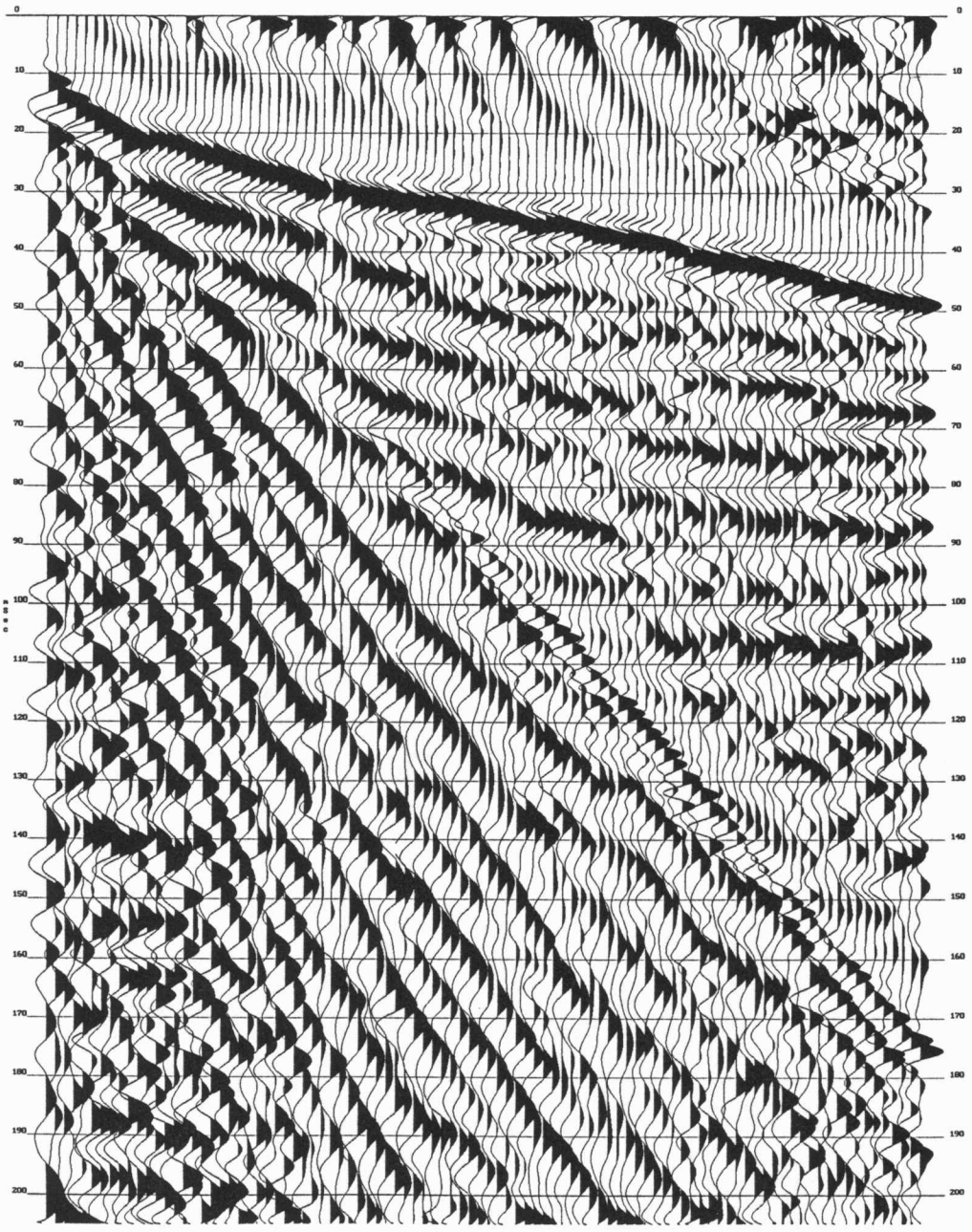
0
10
20
30
40
50
60
70
80
90
100
110
120
130
140
150
160
170
180
190
200

Figure 2b

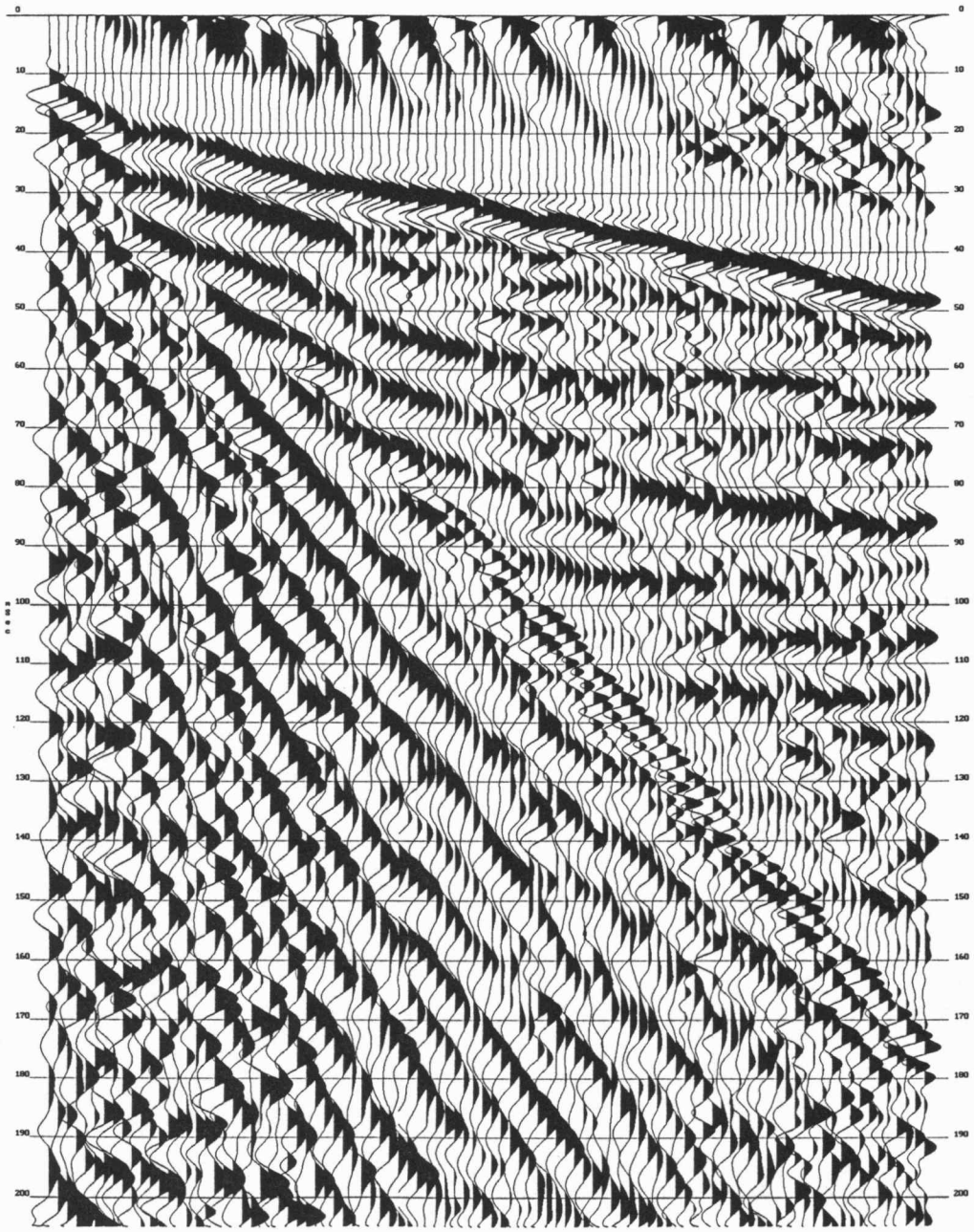
0
10
20
30
40
50
60
70
80
90
100
110
120
130
140
150
160
170
180
190
200

Figure 2c

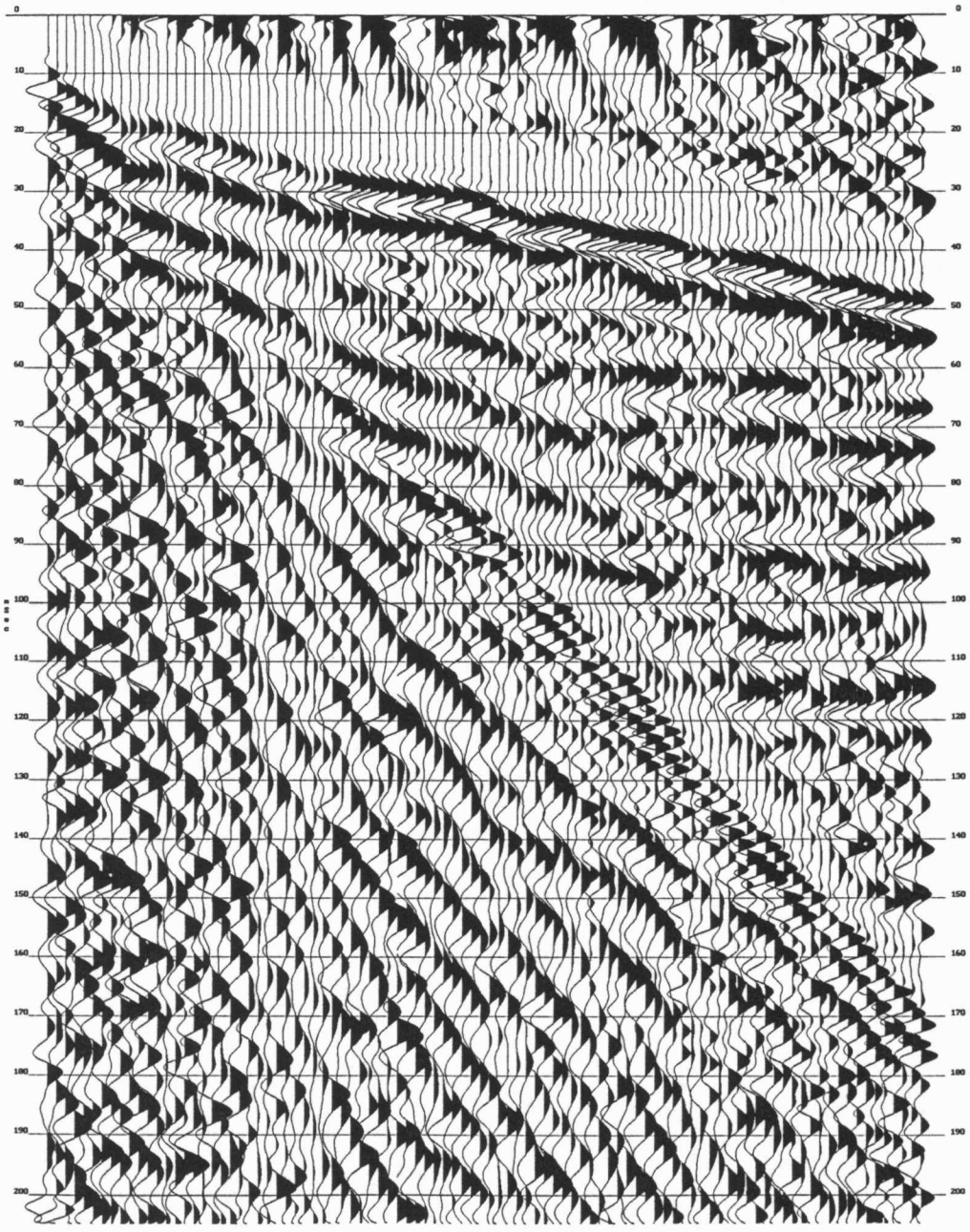
0
10
20
30
40
50
60
70
80
90
100
110
120
130
140
150
160
170
180
190
200
msec

Figure 2d

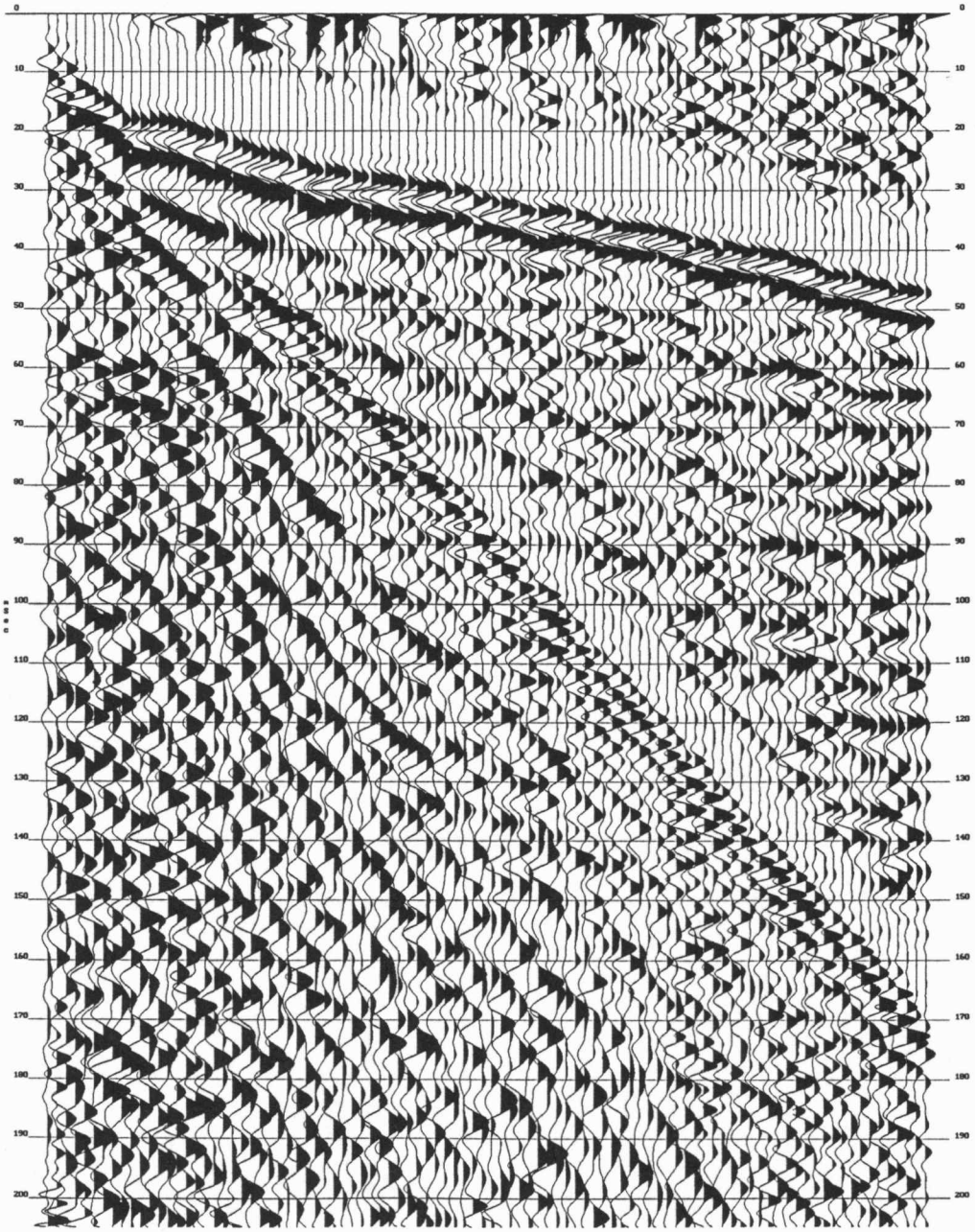
0
10
20
30
40
50
60
70
80
90
100
110
120
130
140
150
160
170
180
190
200

Figure 3a

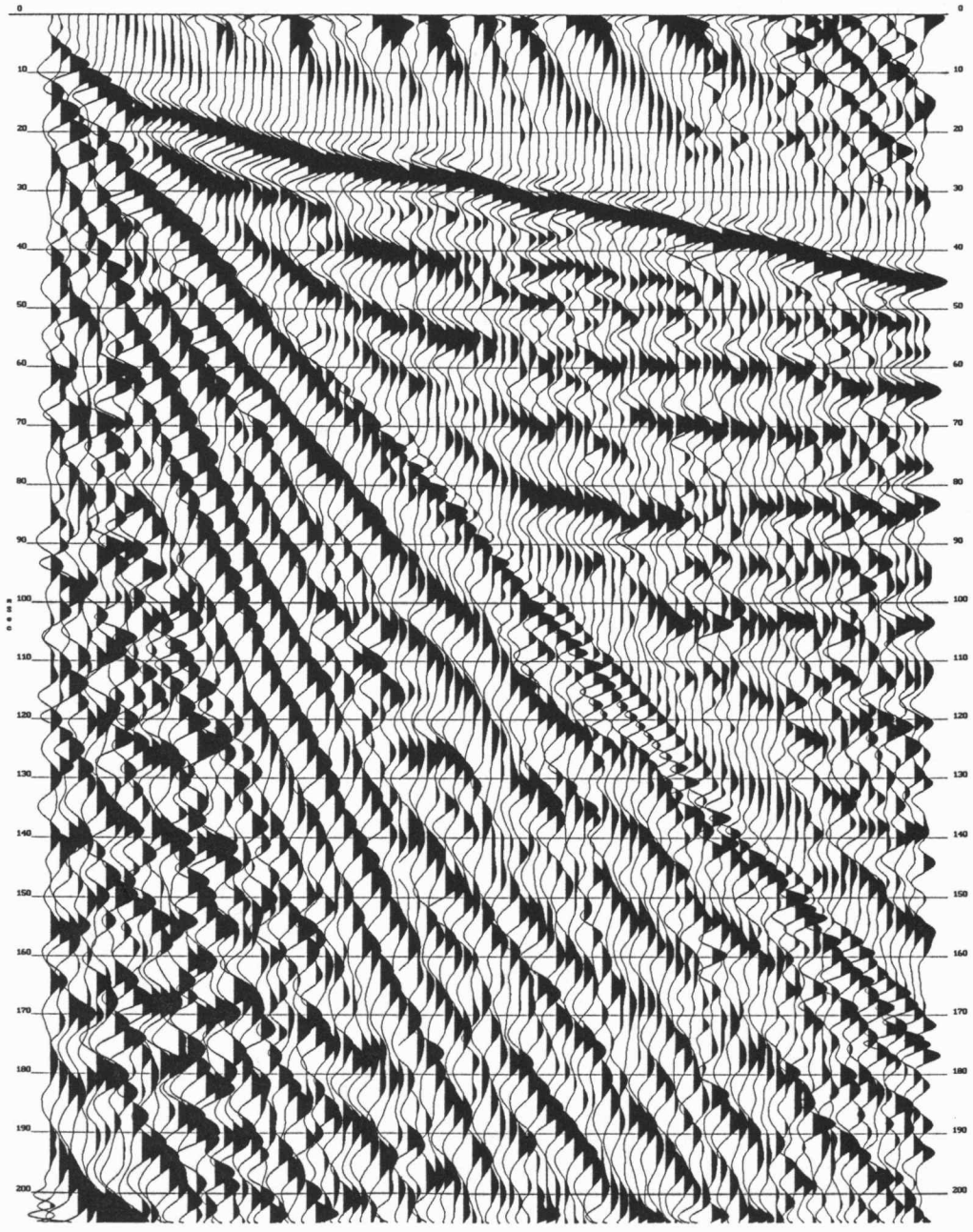
0
10
20
30
40
50
60
70
80
90
100
110
120
130
140
150
160
170
180
190
200

Figure 3b

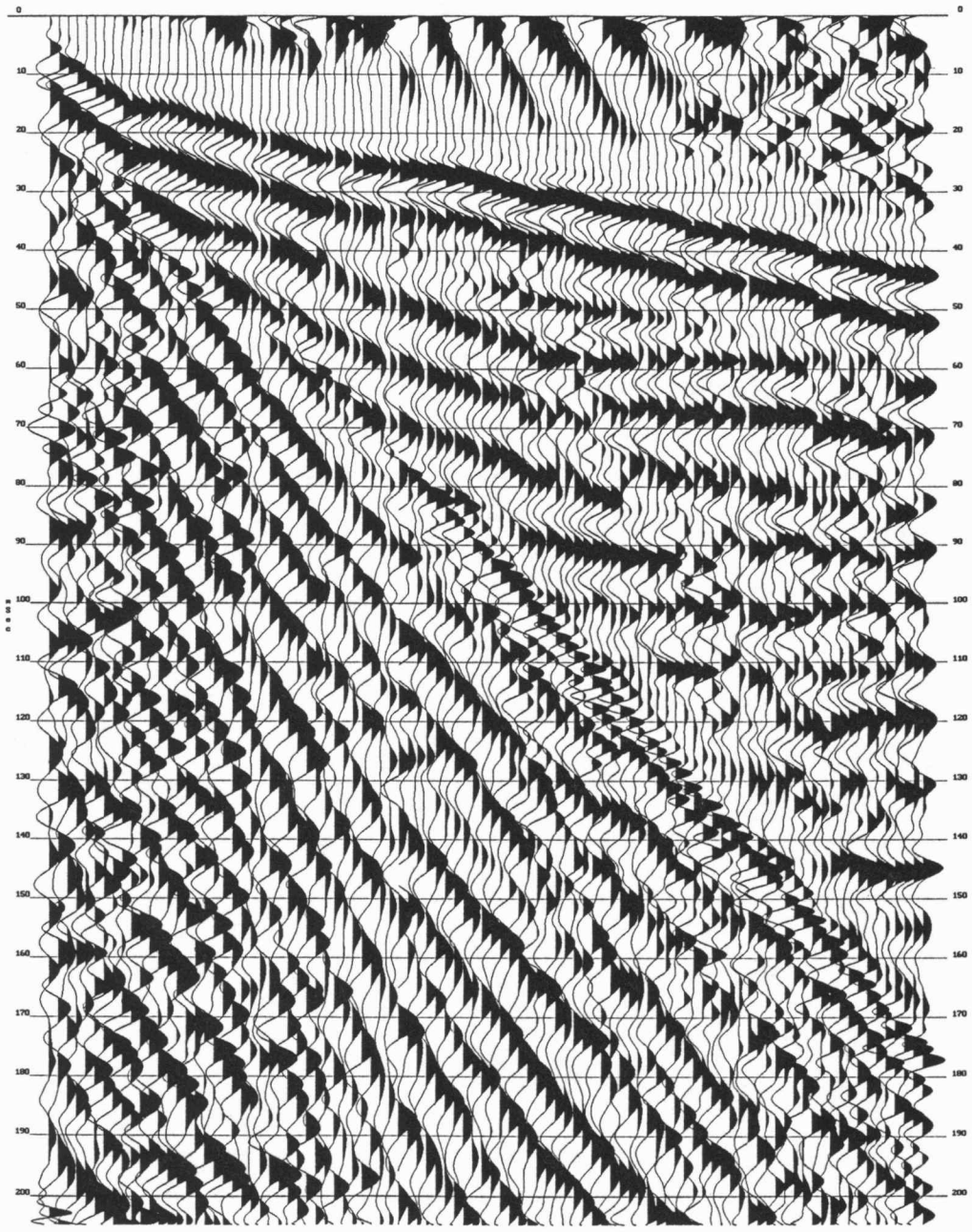
0
10
20
30
40
50
60
70
80
90
100
110
120
130
140
150
160
170
180
190
200

Figure 3c

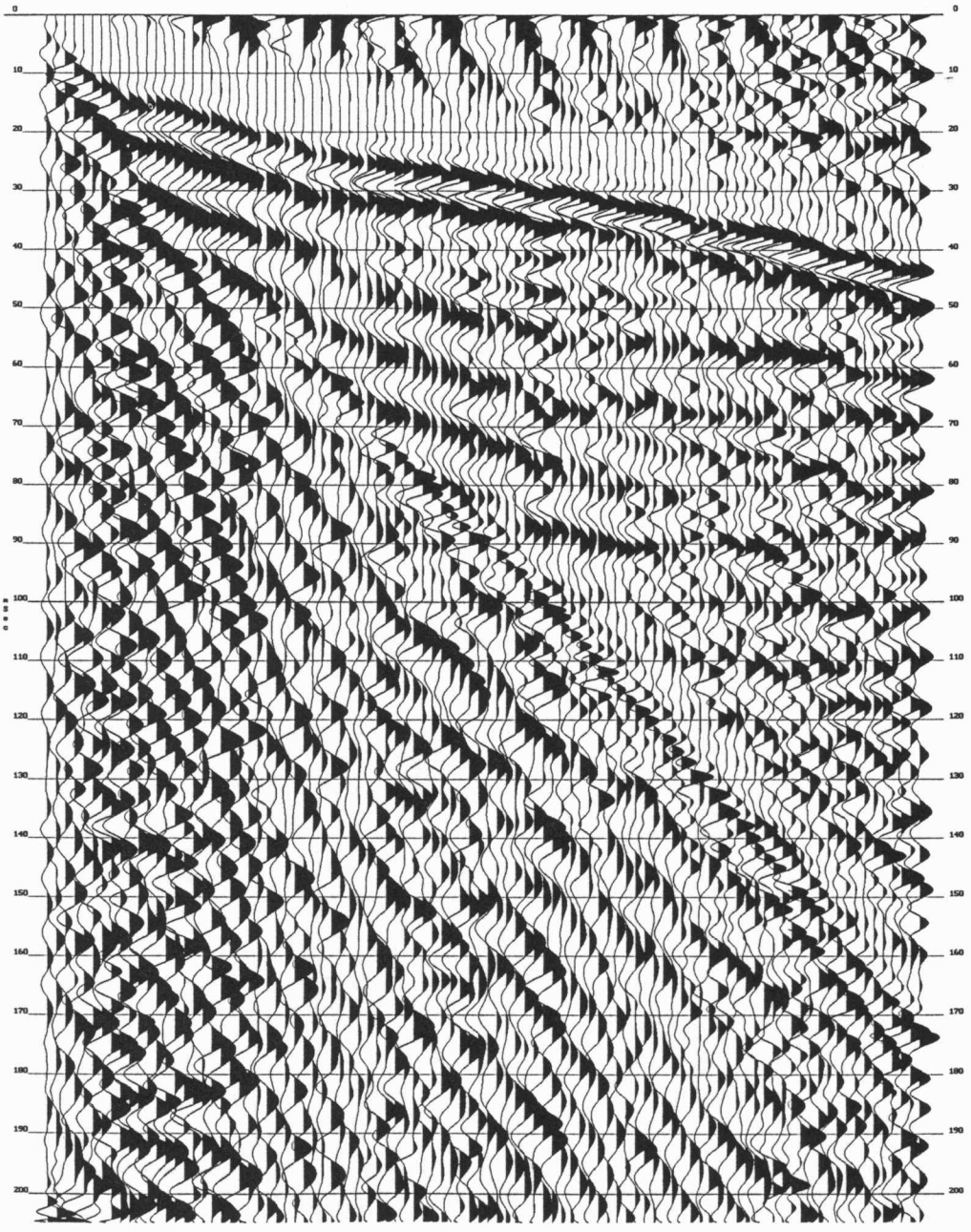
0
10
20
30
40
50
60
70
80
90
100
110
120
130
140
150
160
170
180
190
200

Figure 3d

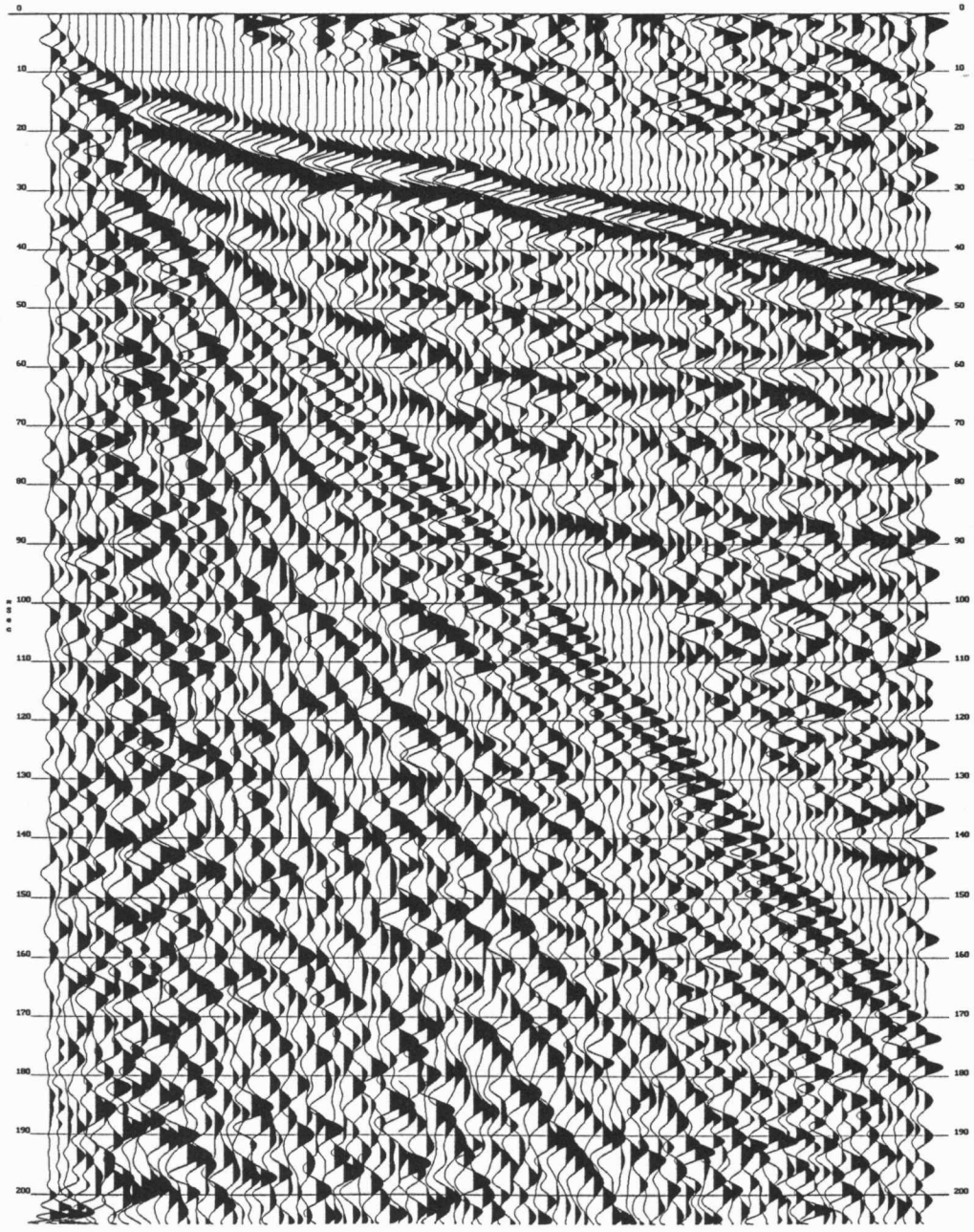
0
10
20
30
40
50
60
70
80
90
100
110
120
130
140
150
160
170
180
190
200

Figure 4a

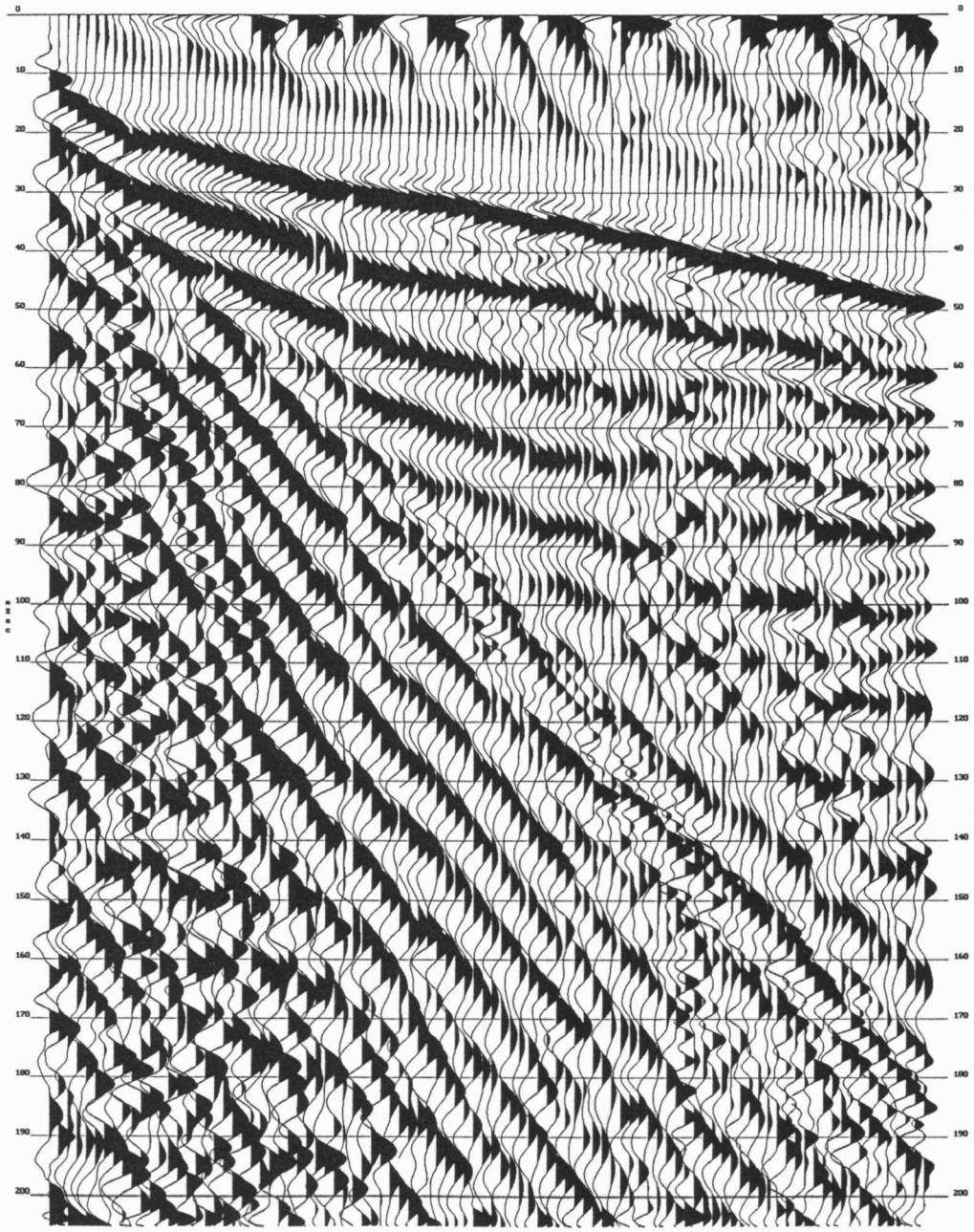
0
10
20
30
40
50
60
70
80
90
100
110
120
130
140
150
160
170
180
190
200
msec

Figure 4b

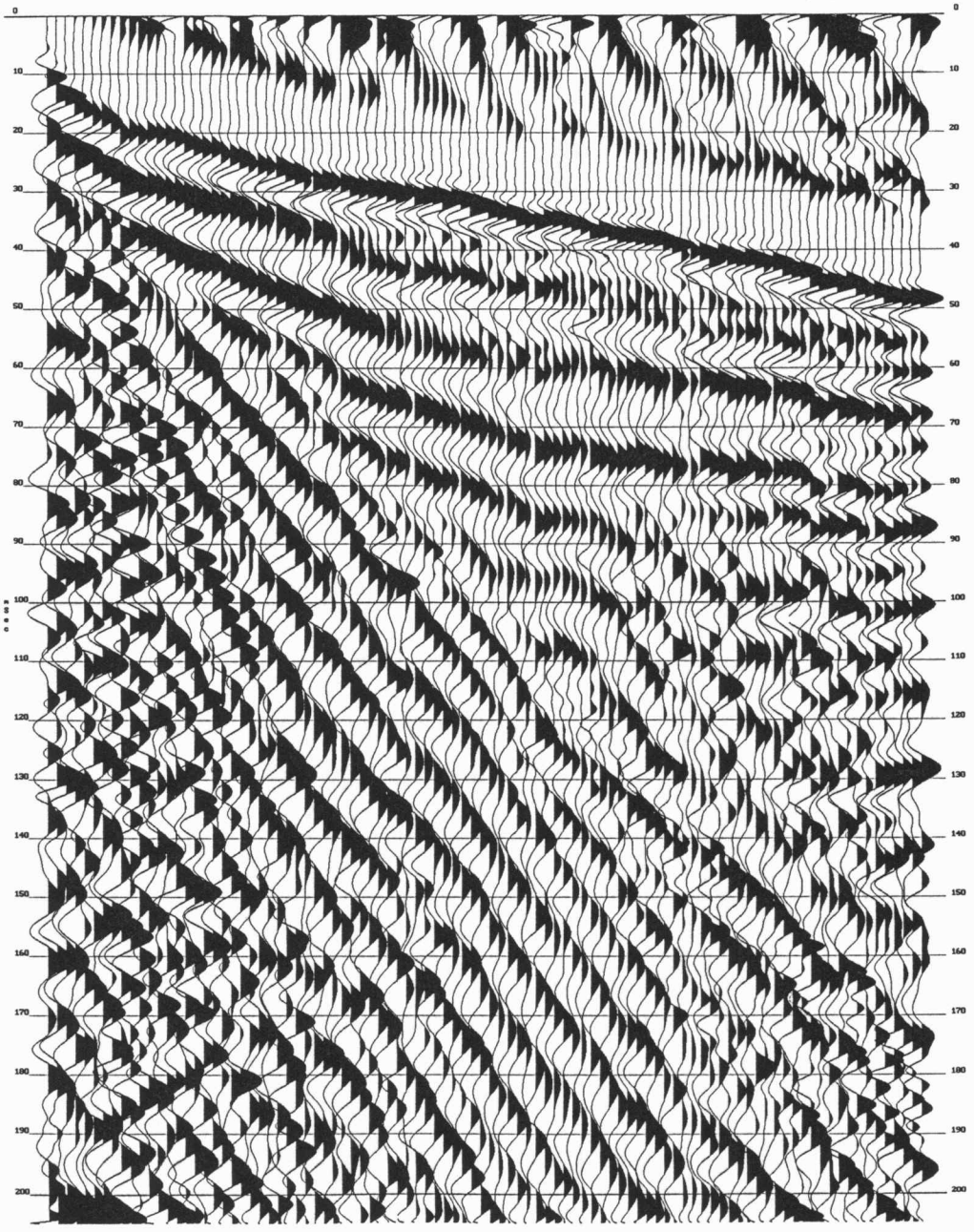
0
10
20
30
40
50
60
70
80
90
100
110
120
130
140
150
160
170
180
190
200

Figure 4c

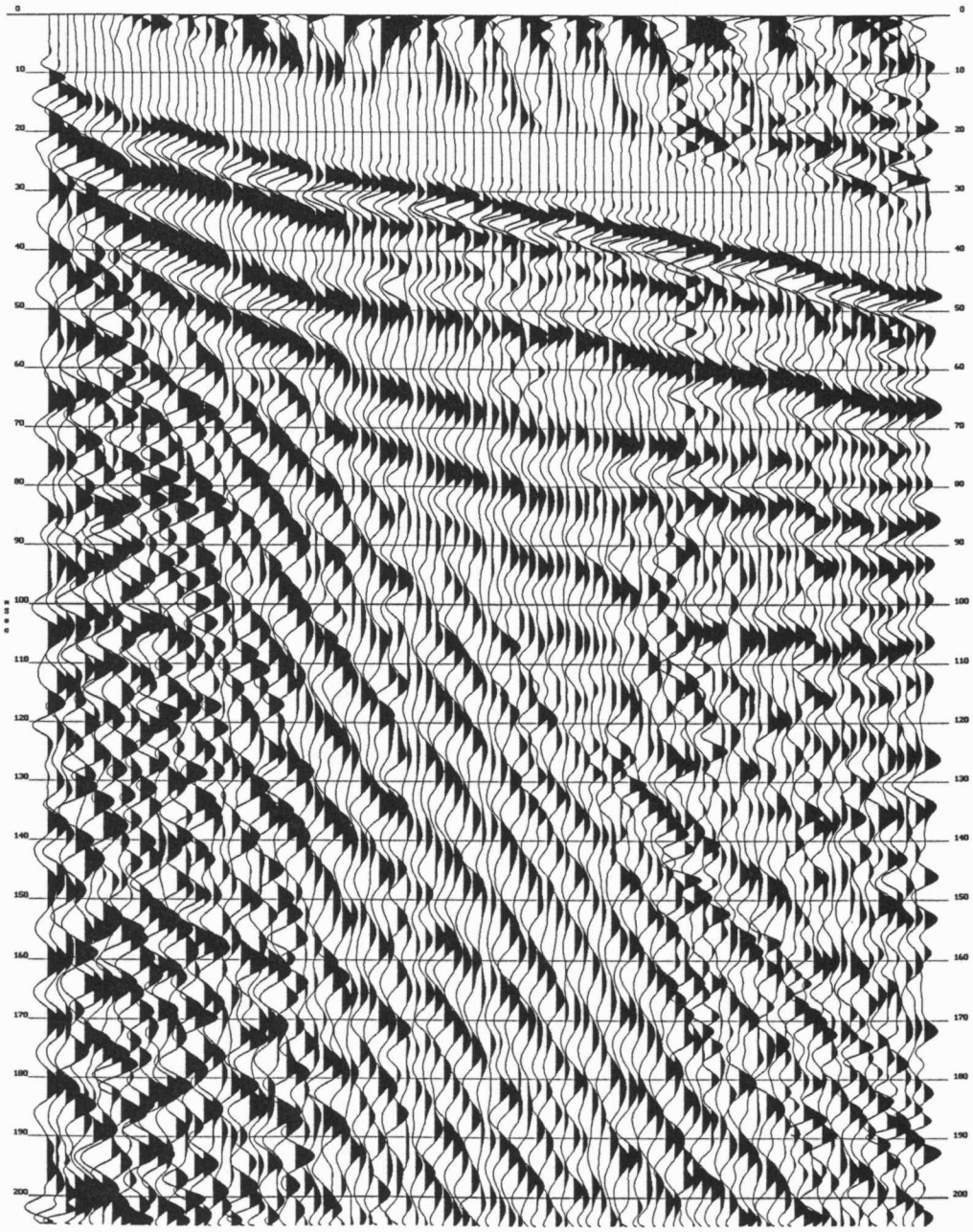
0
10
20
30
40
50
60
70
80
90
100
110
120
130
140
150
160
170
180
190
200

Figure 4d

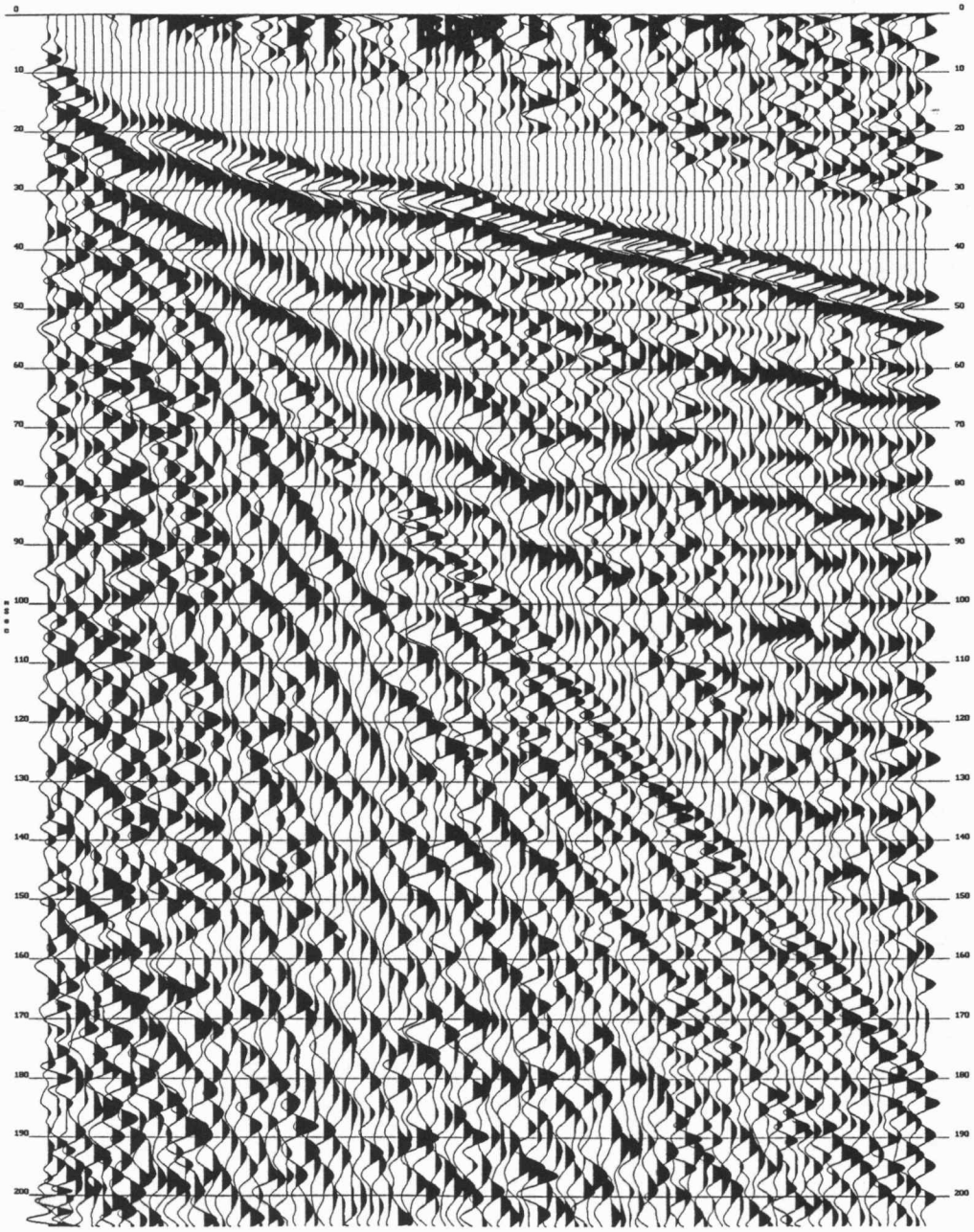
0
10
20
30
40
50
60
70
80
90
100
110
120
130
140
150
160
170
180
190
200

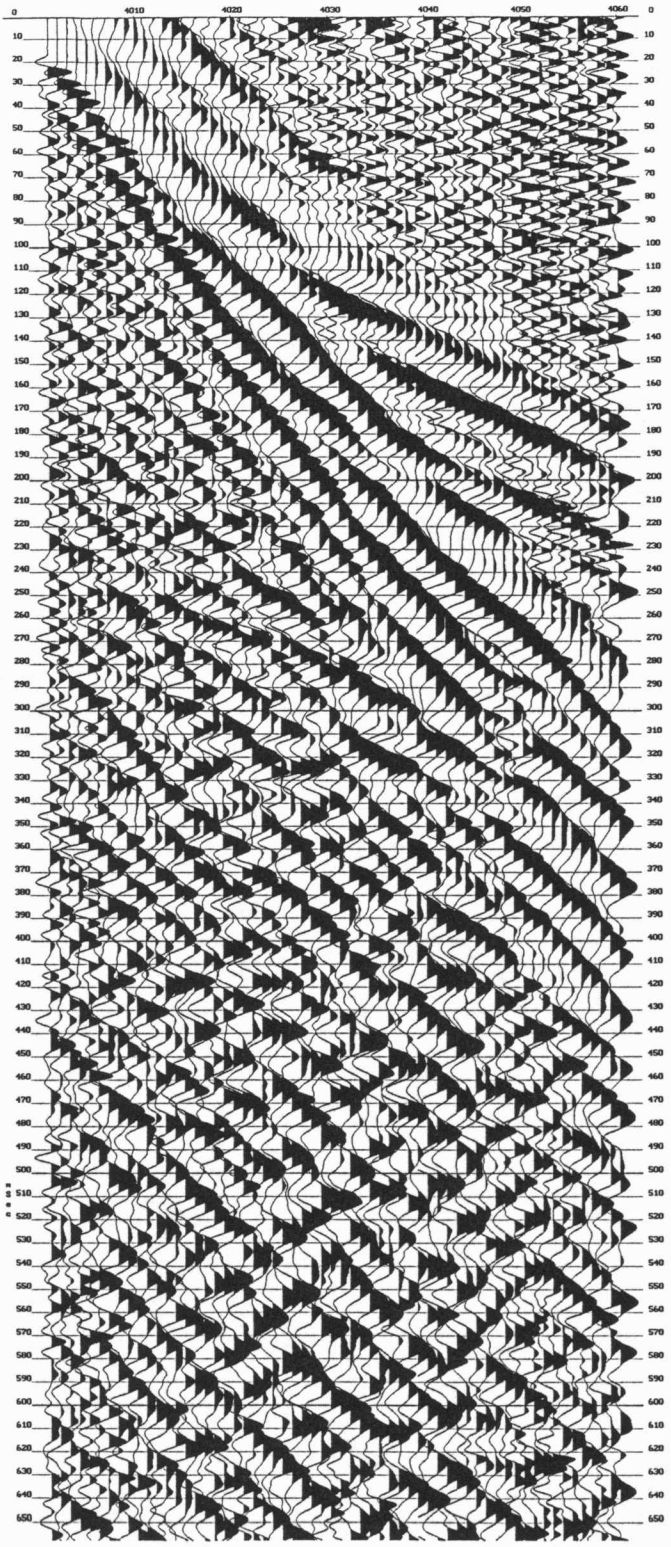

Figure 5

8'S

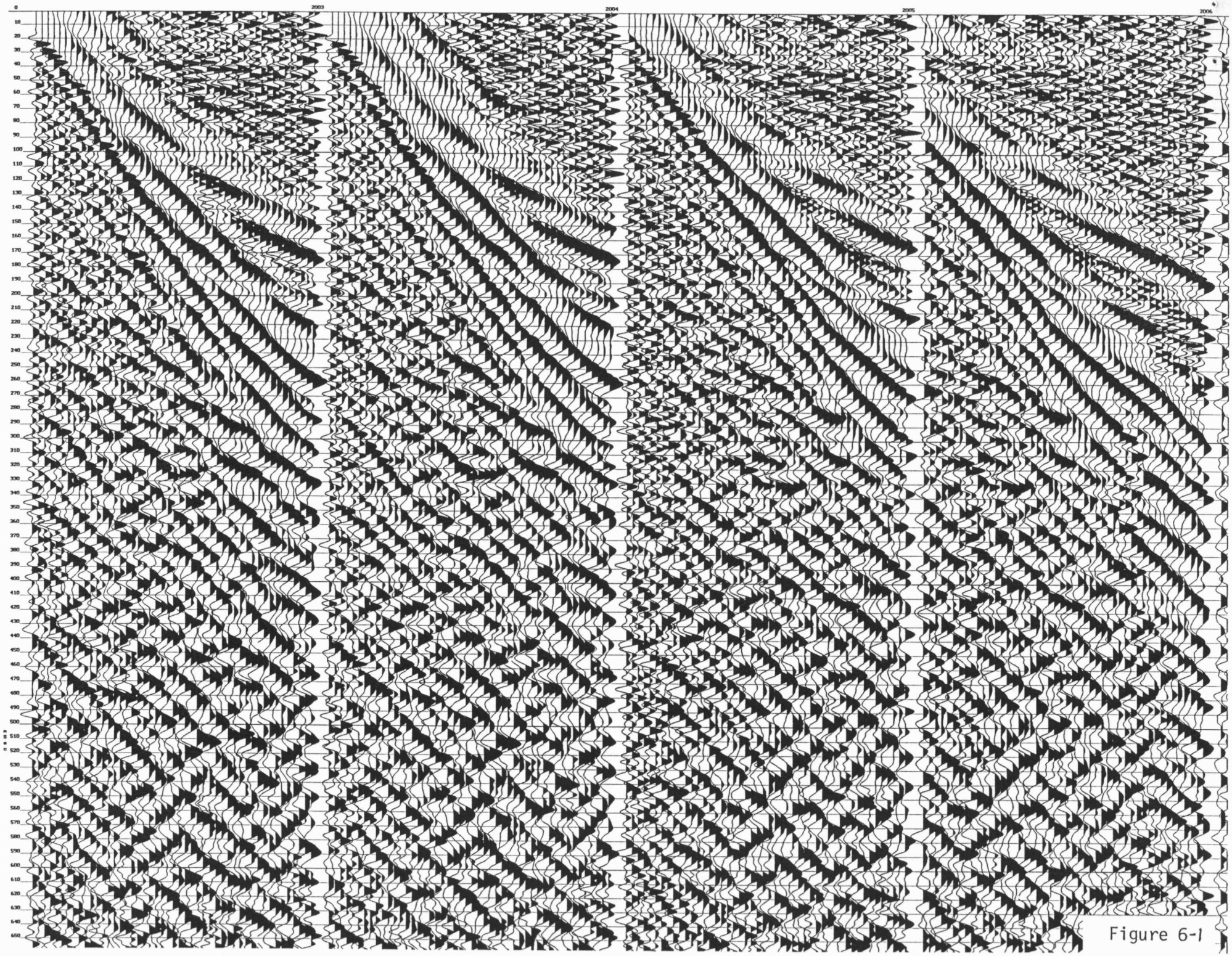

Figure 6-1

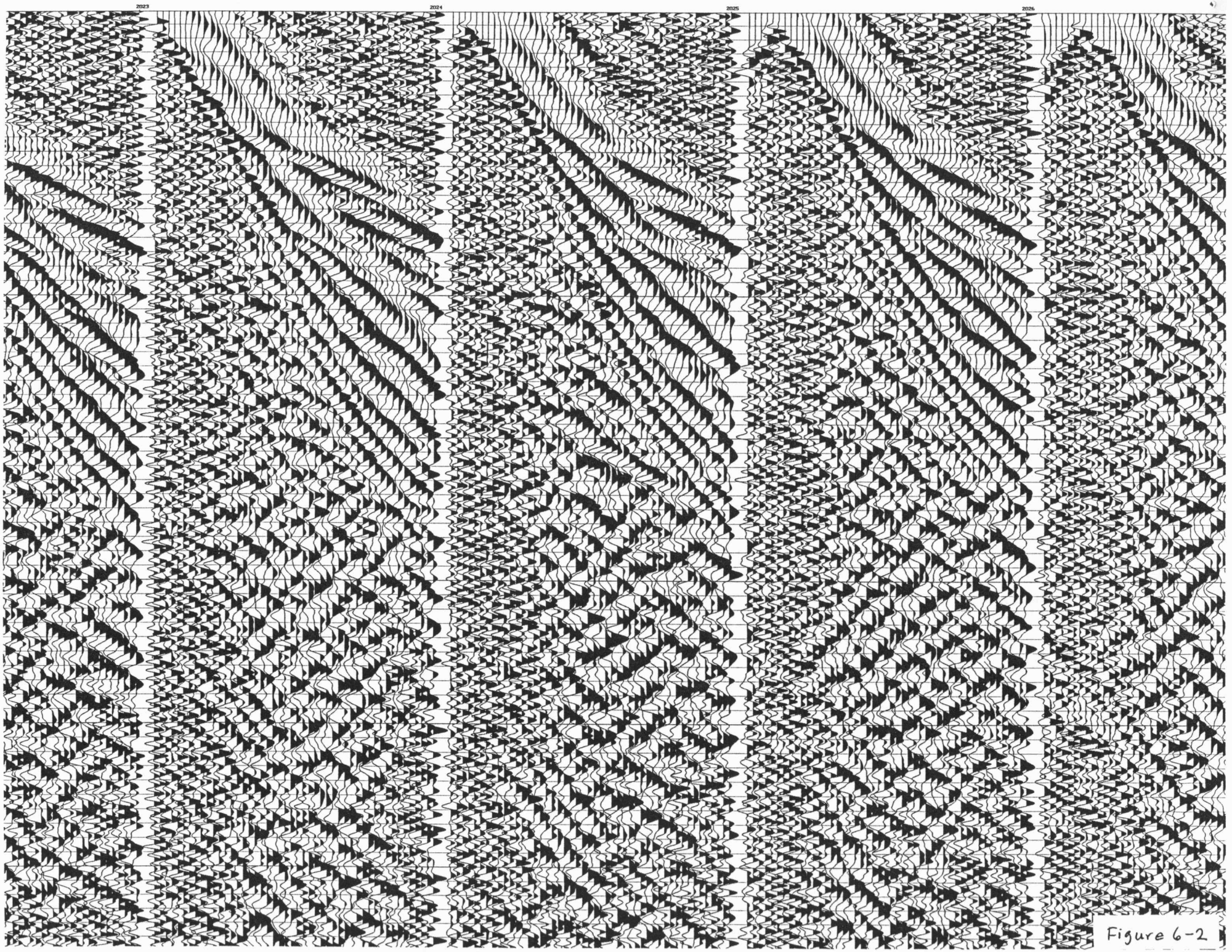

Figure 6-2

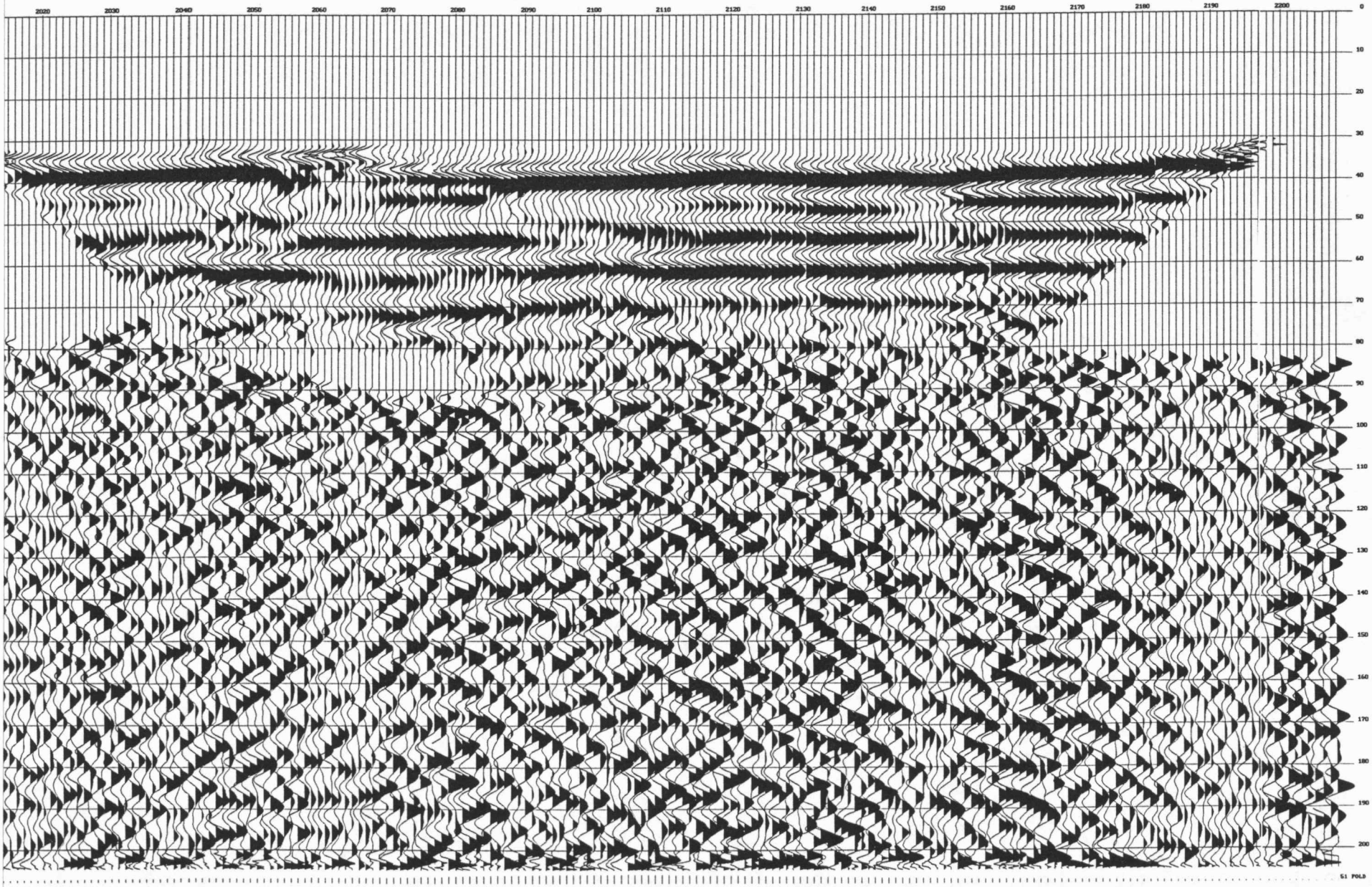
2020
2030
2040
2050
2060
2070
2080
2090
2100
2110
2120
2130
2140
2150
2160
2170
2180
2190
2200
0
10
20
30
40
50
60
70
80
90
100
110
120
130
140
150
160
170
180
190
200
51 POLS

Figure 8

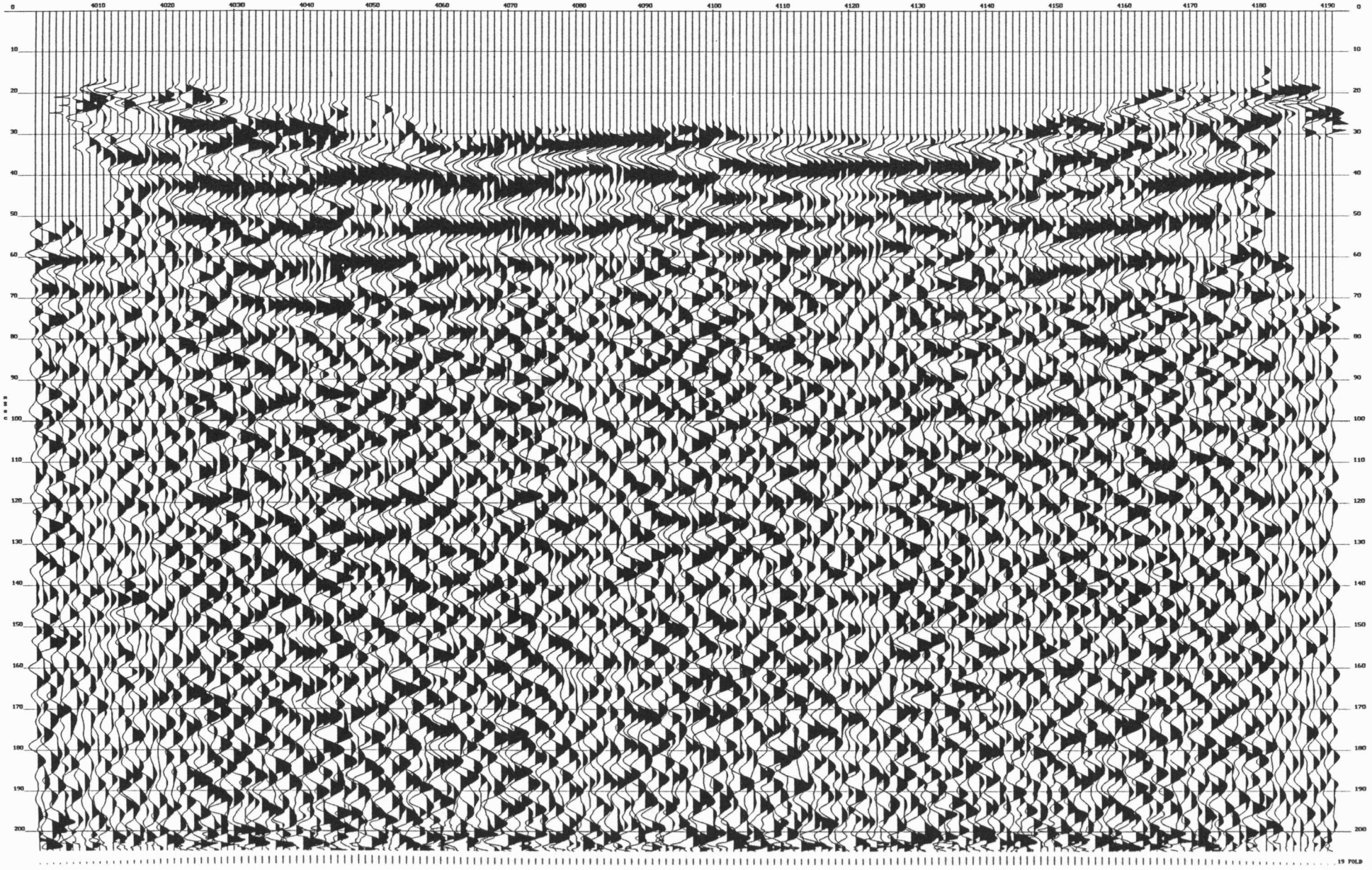
4010
4020
4030
4040
4050
4060
4070
4080
4090
4100
4110
4120
4130
4140
4150
4160
4170
4180
4190
19 FOLD

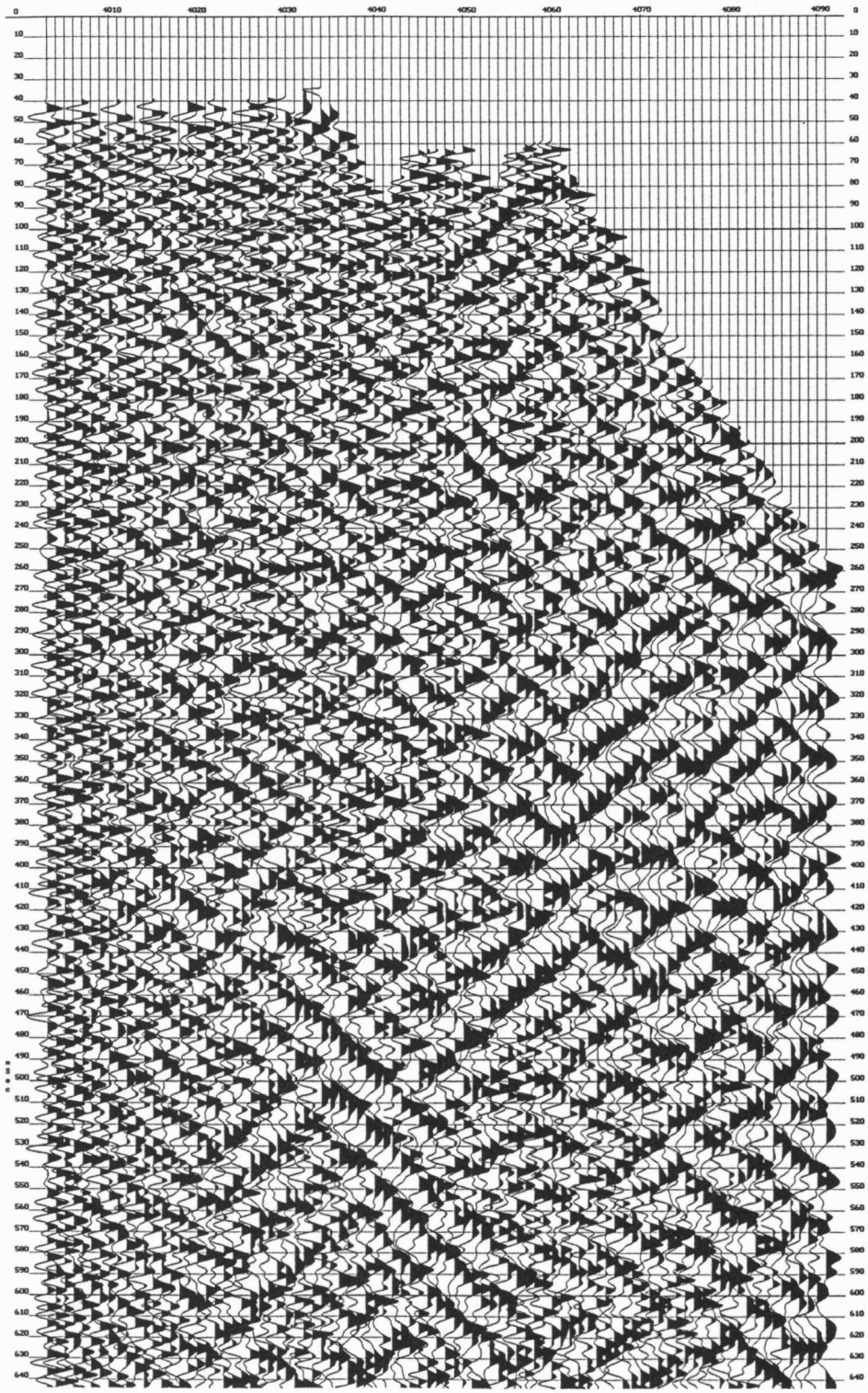
0
4010
4020
4030
4040
4050
4060
4070
4080
4090
0
10
20
30
40
50
60
70
80
90
100
110
120
130
140
150
160
170
180
190
200
210
220
230
240
250
260
270
280
290
300
310
320
330
340
350
360
370
380
390
400
410
420
430
440
450
460
470
480
490
500
510
520
530
540
550
560
570
580
590
600
610
620
630
640

Figure 9

Figure 10a

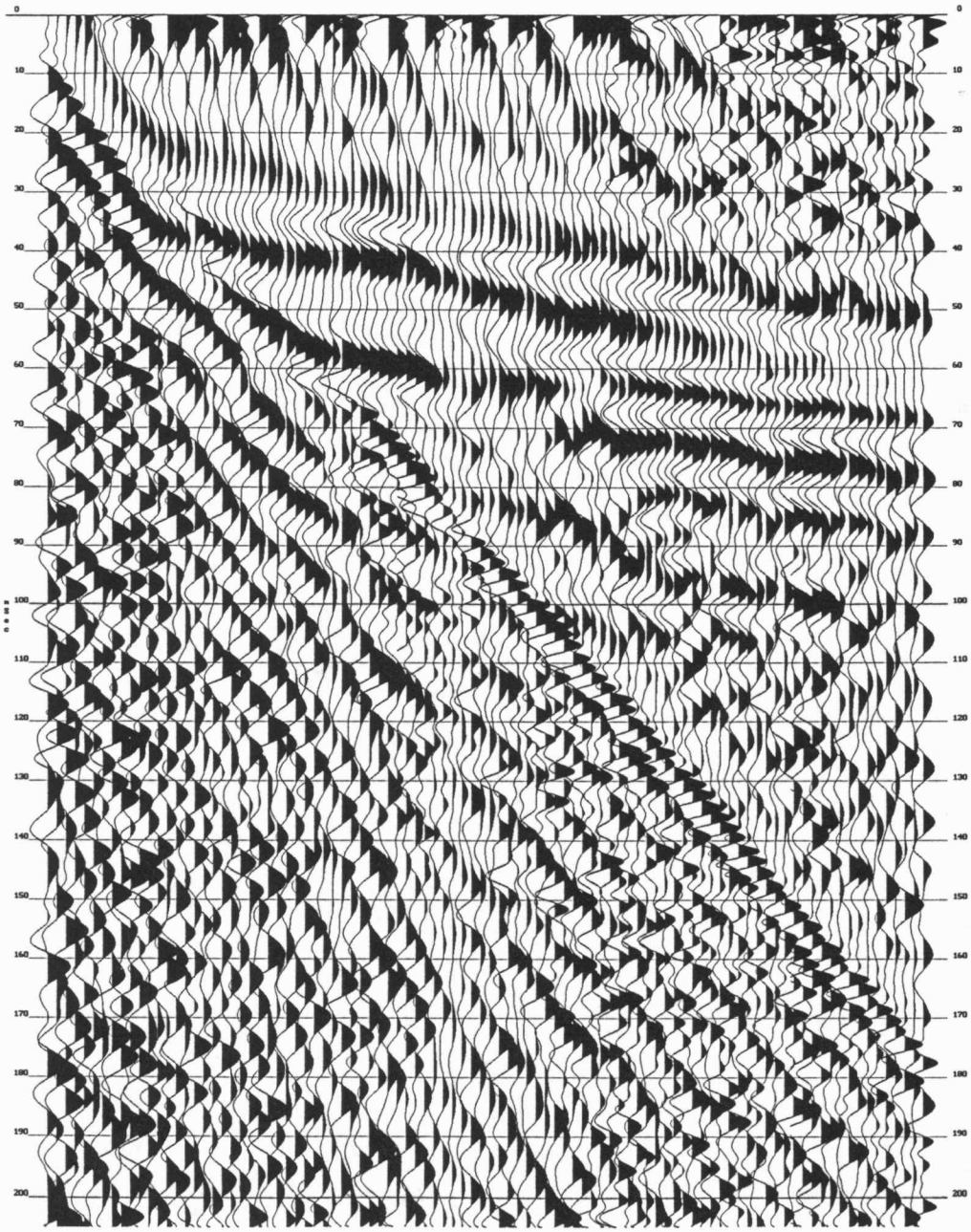
0
10
20
30
40
50
60
70
80
90
100
110
120
130
140
150
160
170
180
190
200
TIME

Figure 10b

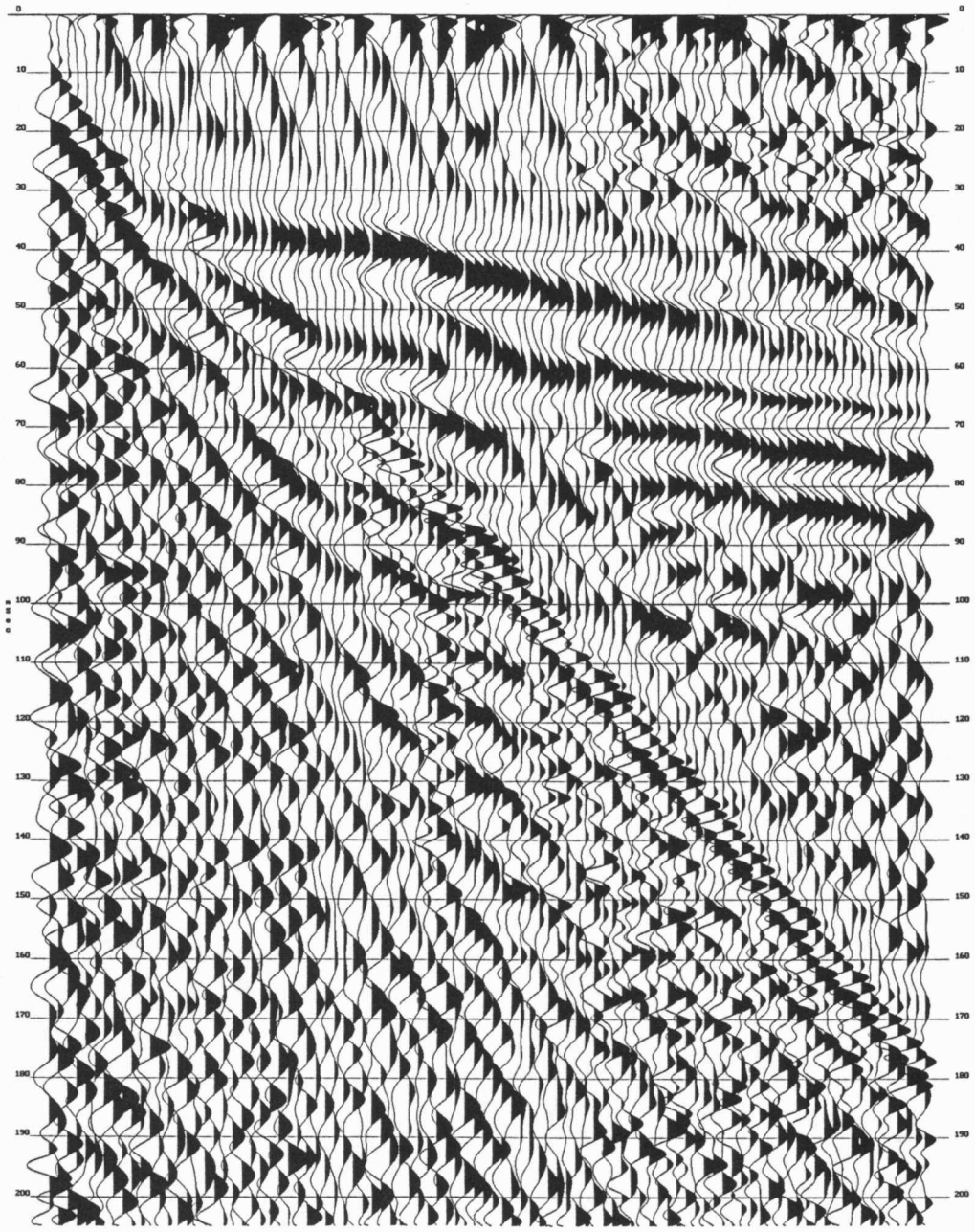
0
10
20
30
40
50
60
70
80
90
100
110
120
130
140
150
160
170
180
190
200

Figure 10c

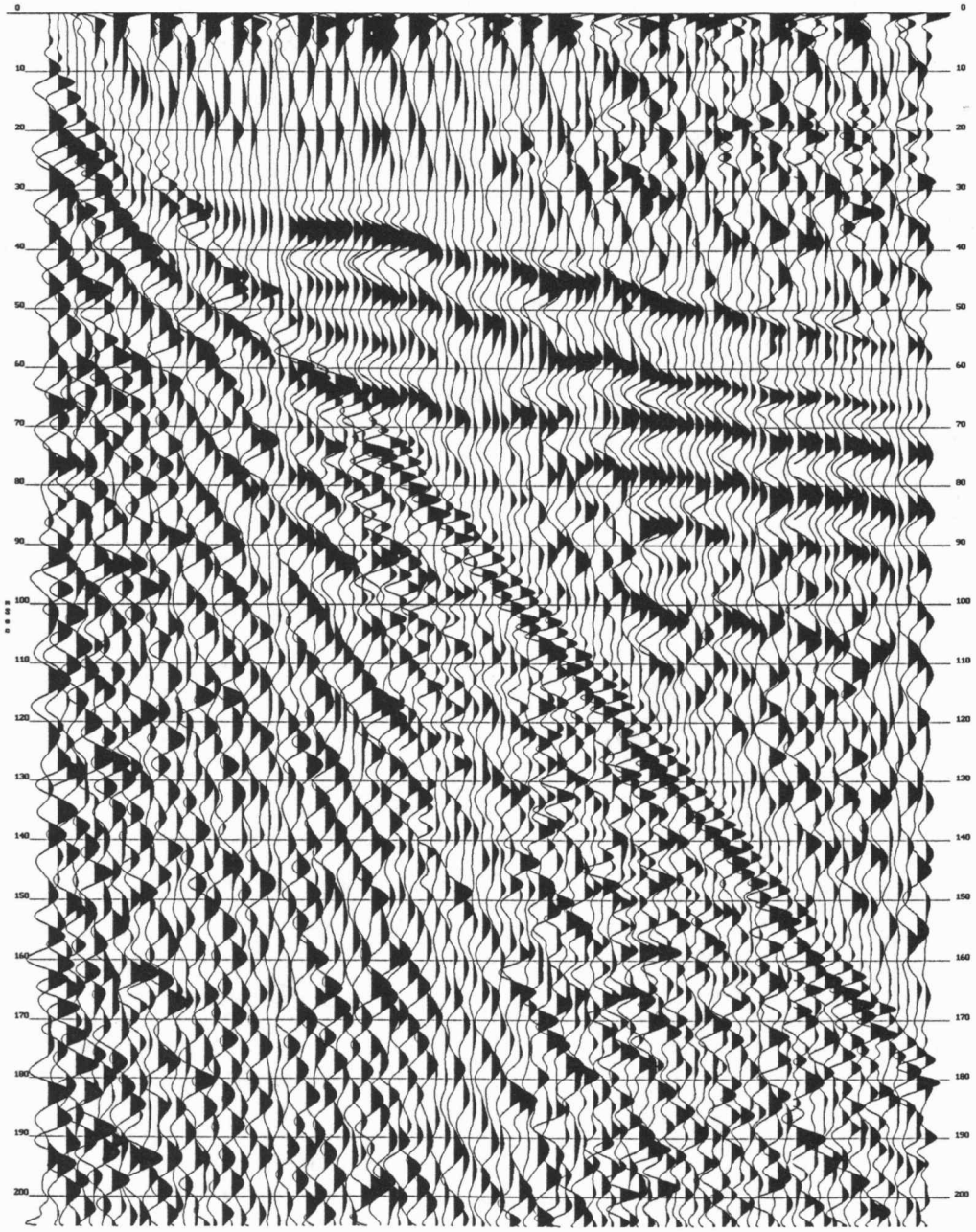
0
10
20
30
40
50
60
70
80
90
100
110
120
130
140
150
160
170
180
190
200

Figure 10d

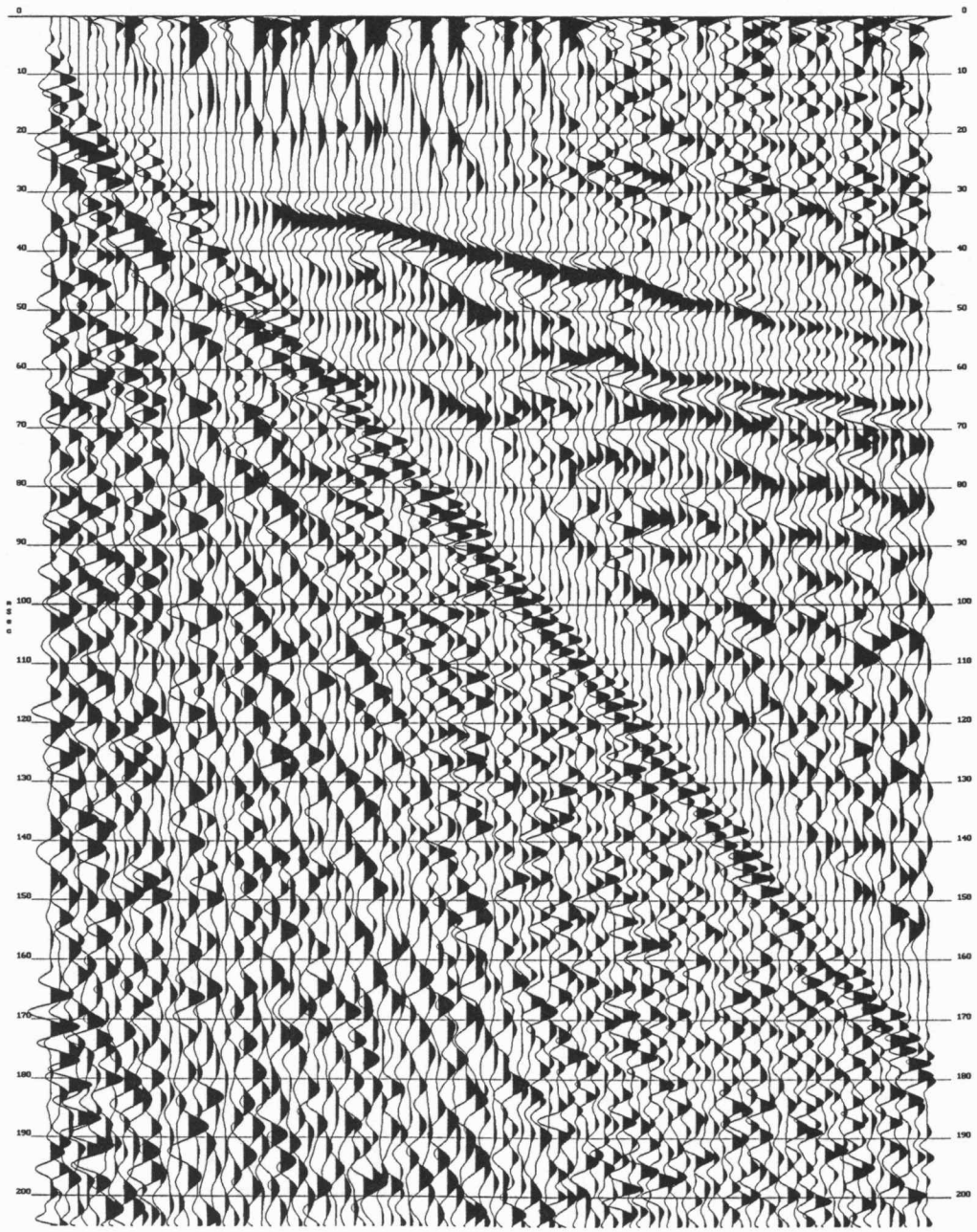
0
10
20
30
40
50
60
70
80
90
100
110
120
130
140
150
160
170
180
190
200

Figure 11a

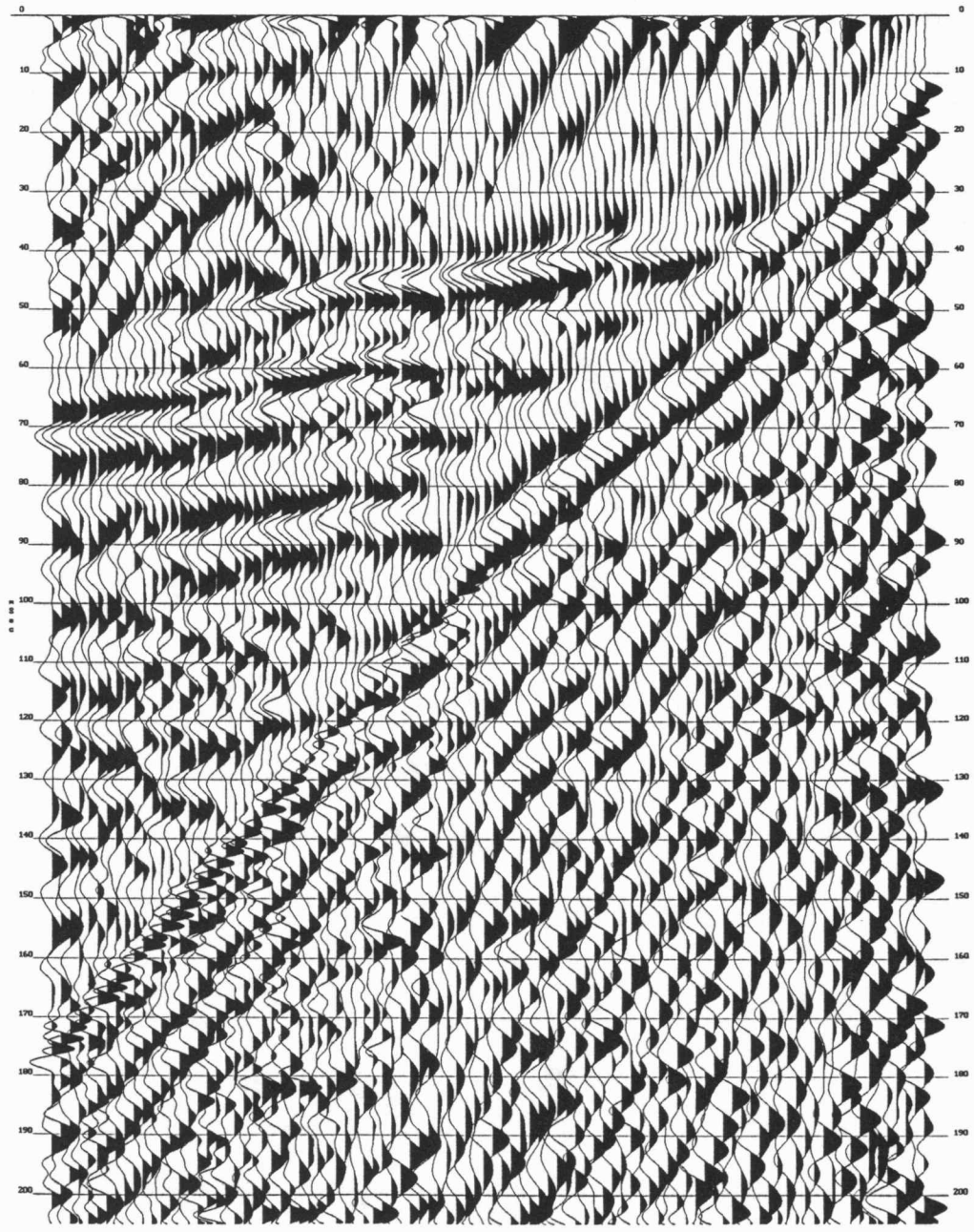
0
10
20
30
40
50
60
70
80
90
100
110
120
130
140
150
160
170
180
190
200

Figure 11b

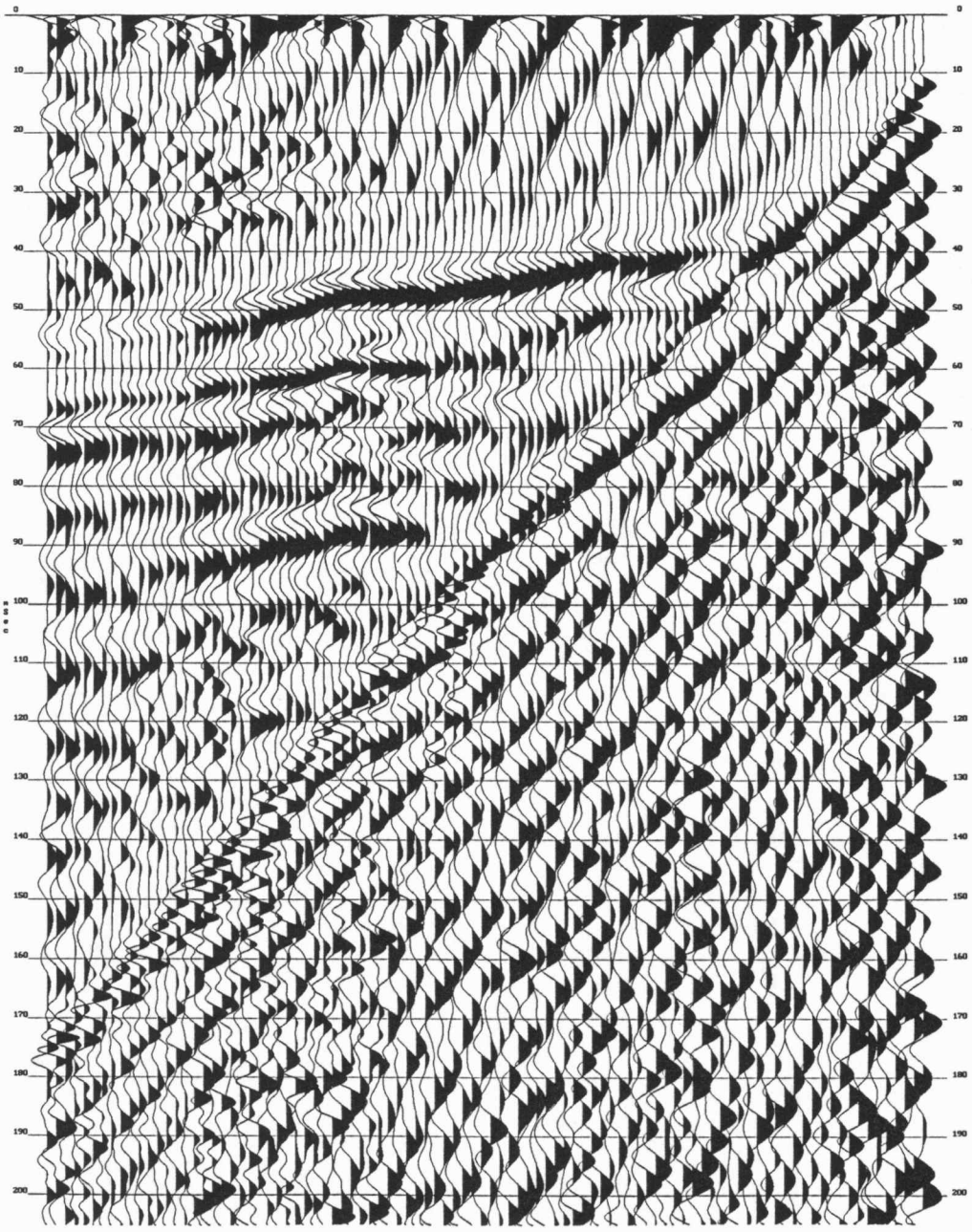
0
10
20
30
40
50
60
70
80
90
100
110
120
130
140
150
160
170
180
190
200

Figure 11c

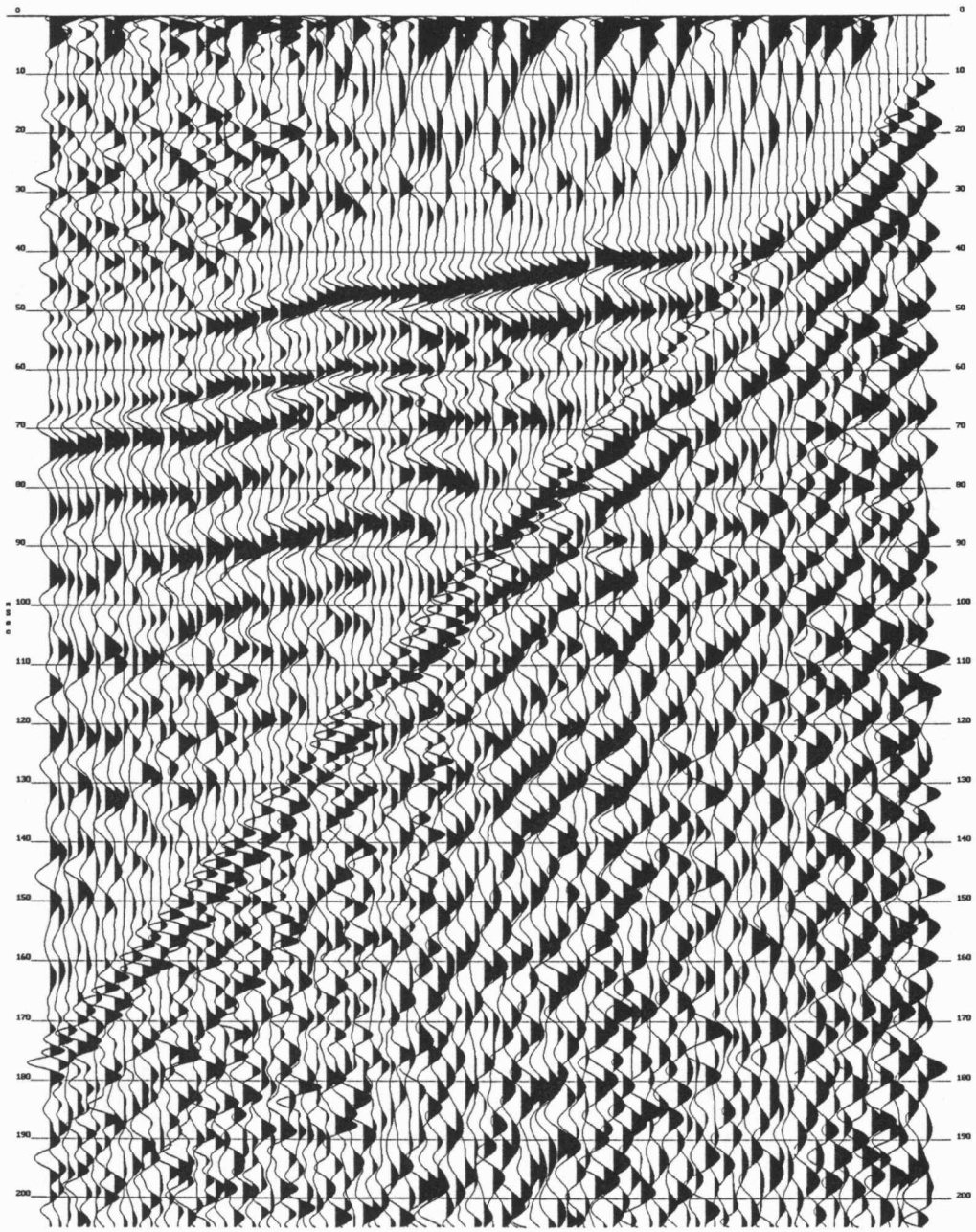
0
10
20
30
40
50
60
70
80
90
100
110
120
130
140
150
160
170
180
190
200

Figure 11d

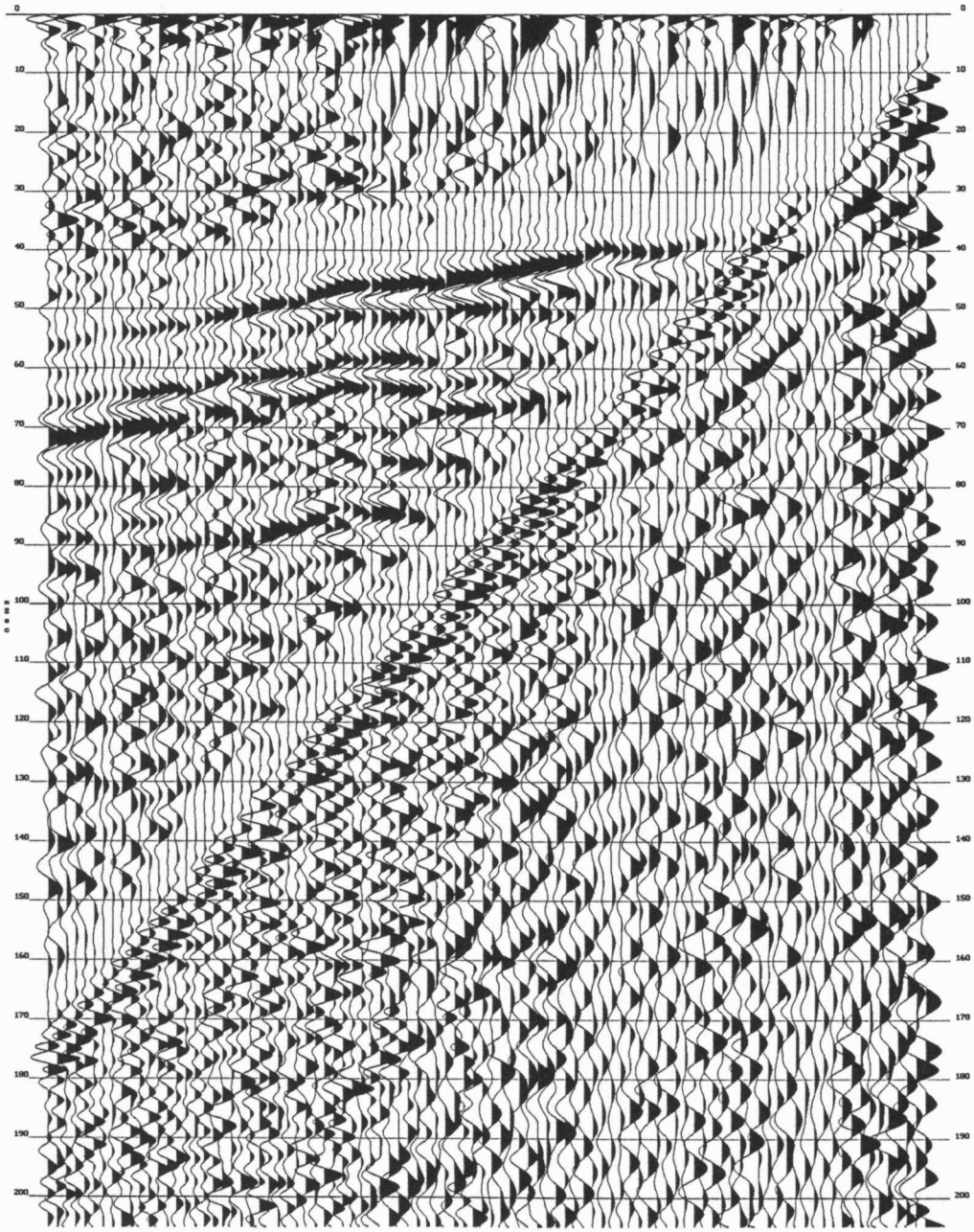
0
10
20
30
40
50
60
70
80
90
100
110
120
130
140
150
160
170
180
190
200

Figure 12a

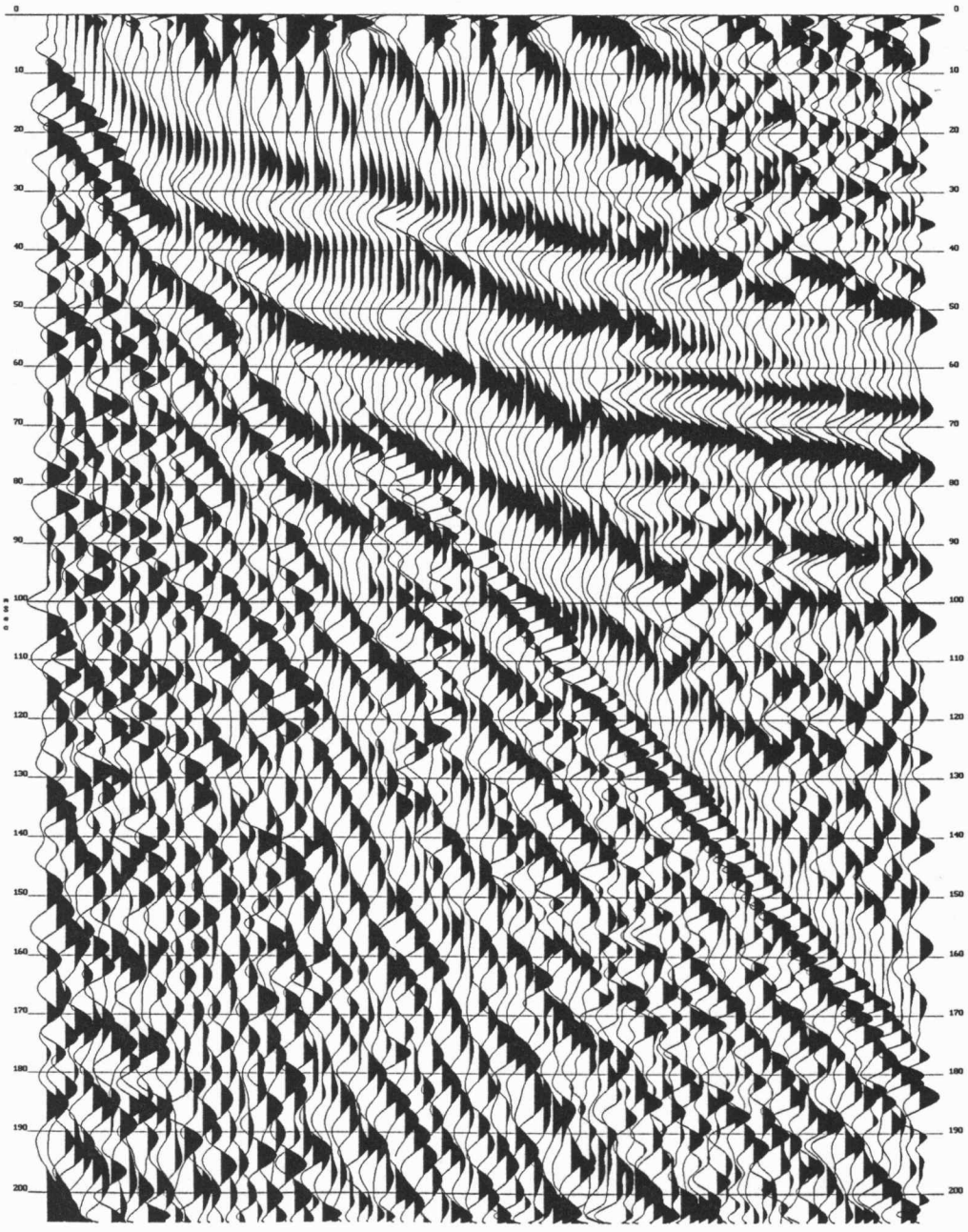
0
10
20
30
40
50
60
70
80
90
100
110
120
130
140
150
160
170
180
190
200

Figure 12b

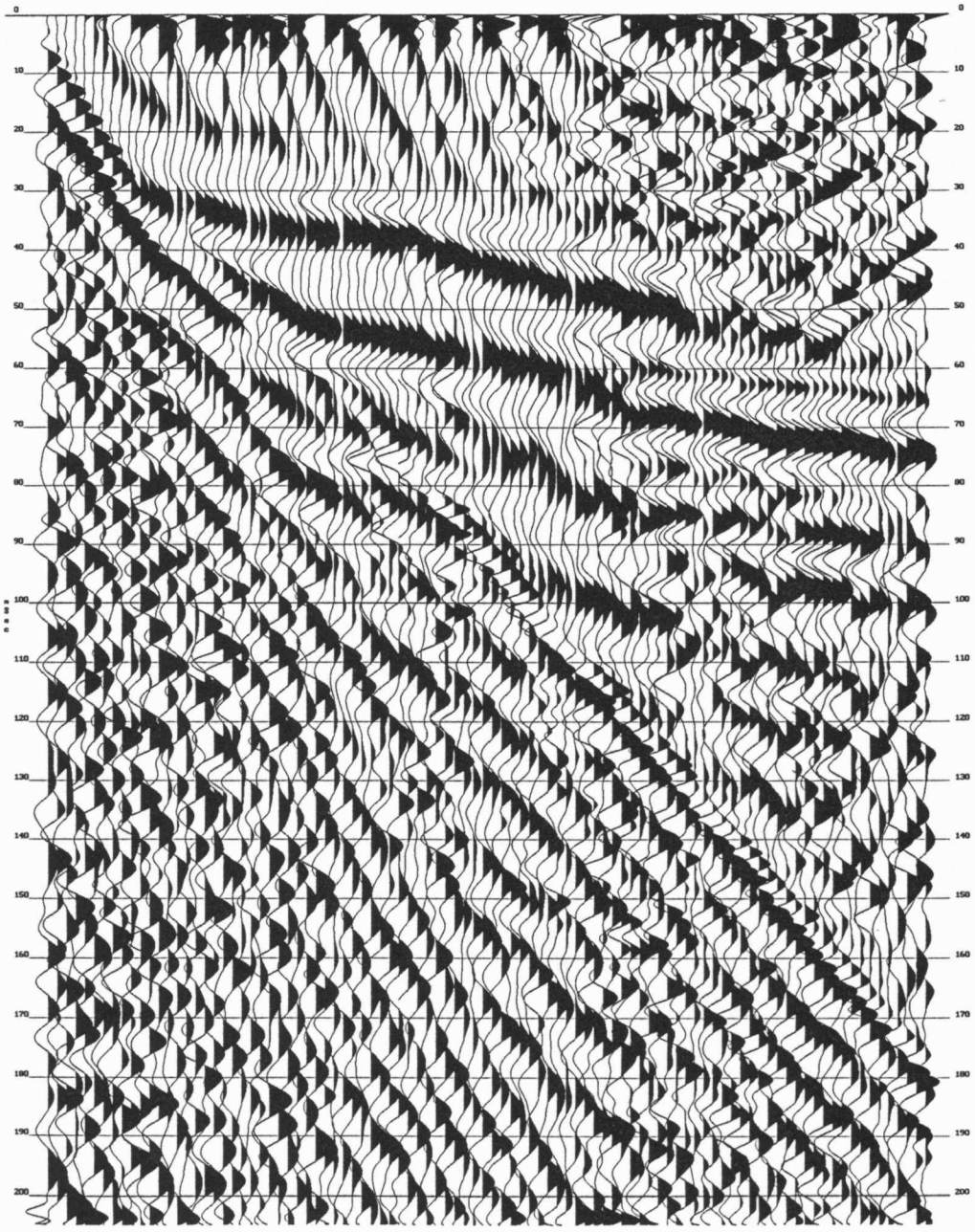
0
10
20
30
40
50
60
70
80
90
100
110
120
130
140
150
160
170
180
190
200

Figure 12c

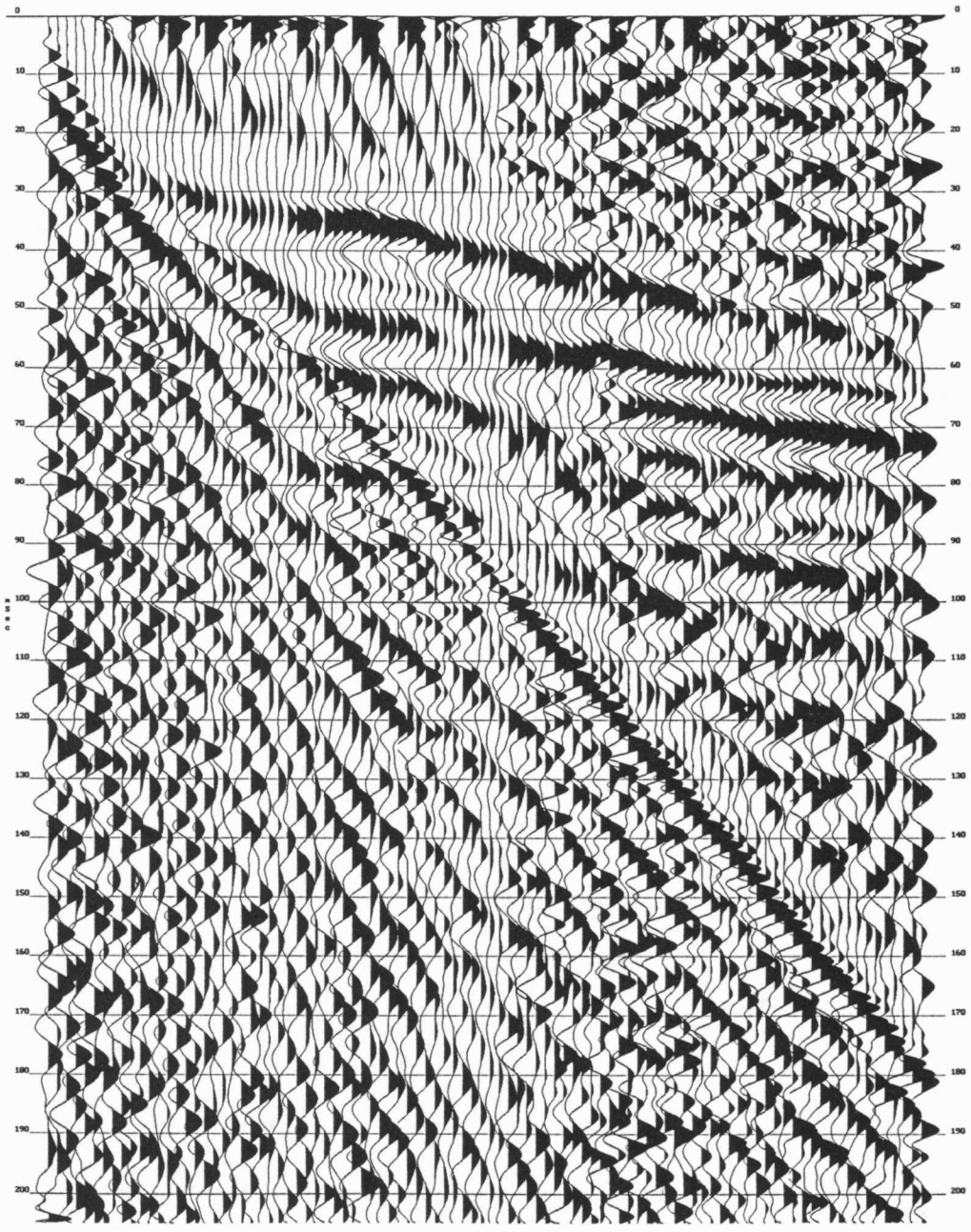
0
10
20
30
40
50
60
70
80
90
100
110
120
130
140
150
160
170
180
190
200

Figure 12d

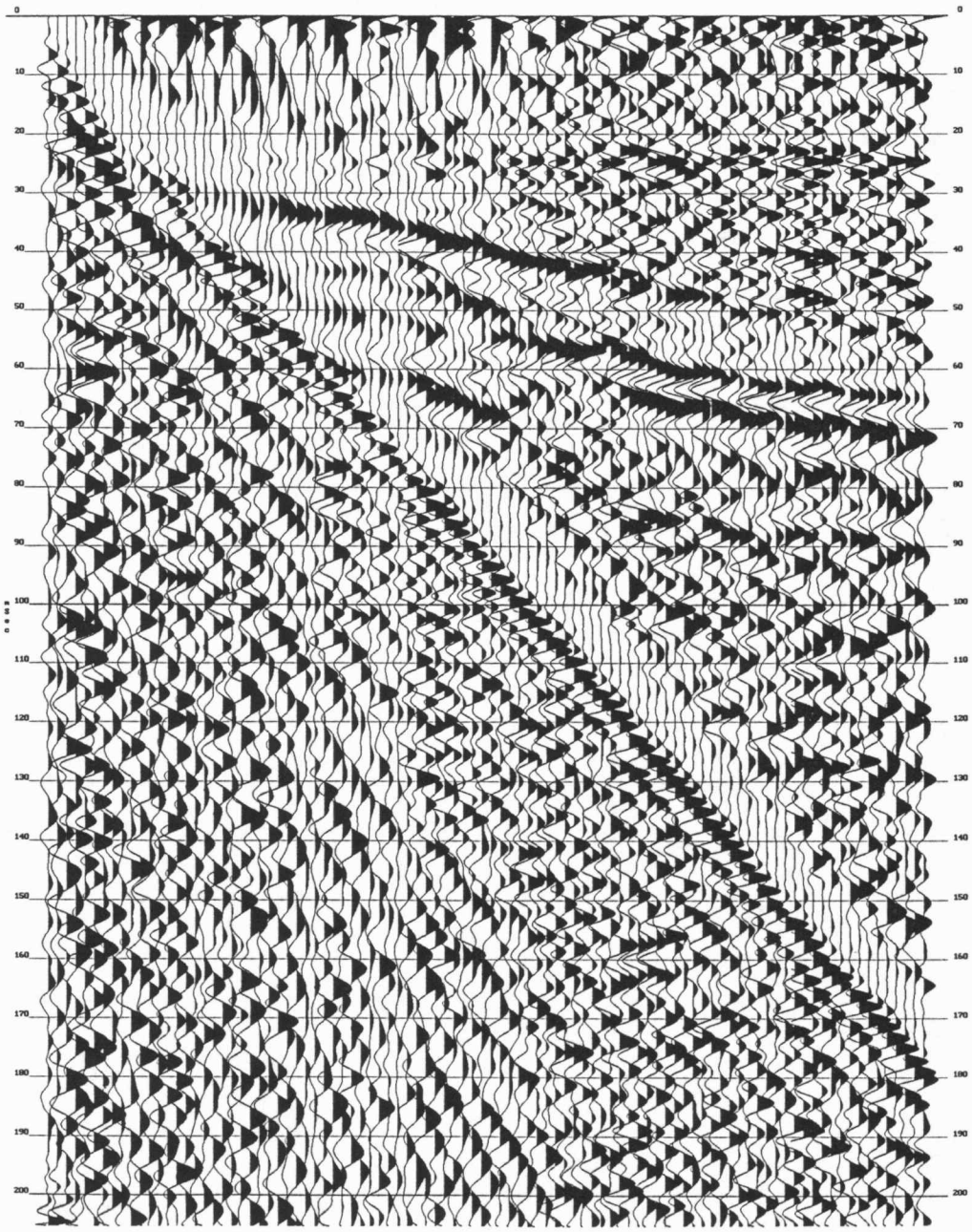
0
10
20
30
40
50
60
70
80
90
100
110
120
130
140
150
160
170
180
190
200

Figure 13a

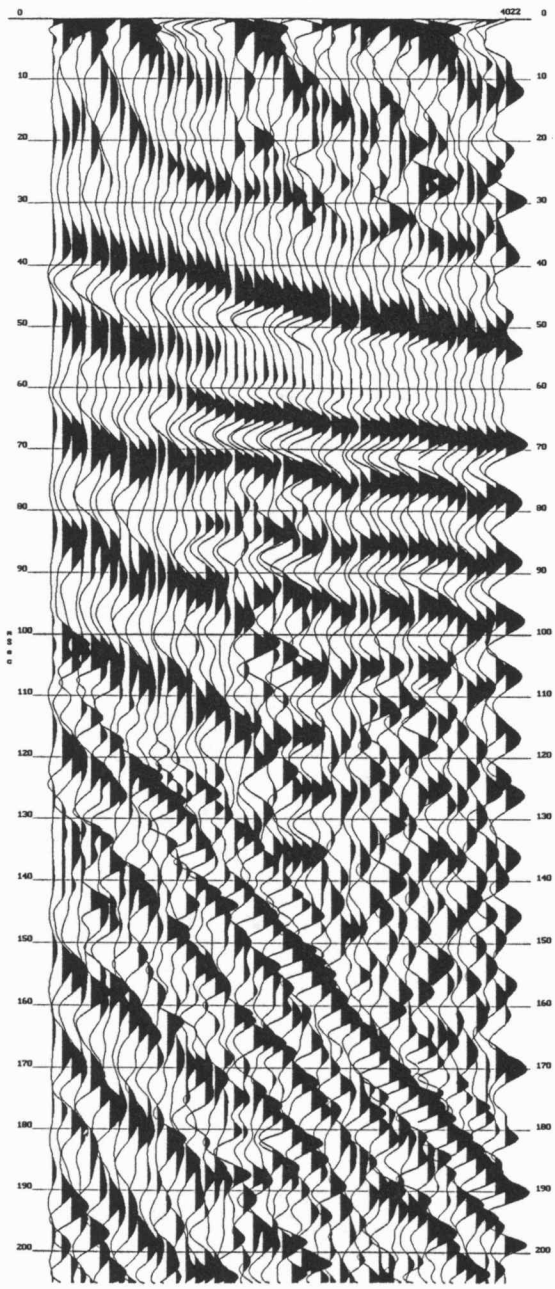
0
4022
0
10
20
30
40
50
60
70
80
90
100
110
120
130
140
150
160
170
180
190
200

Figure 13b

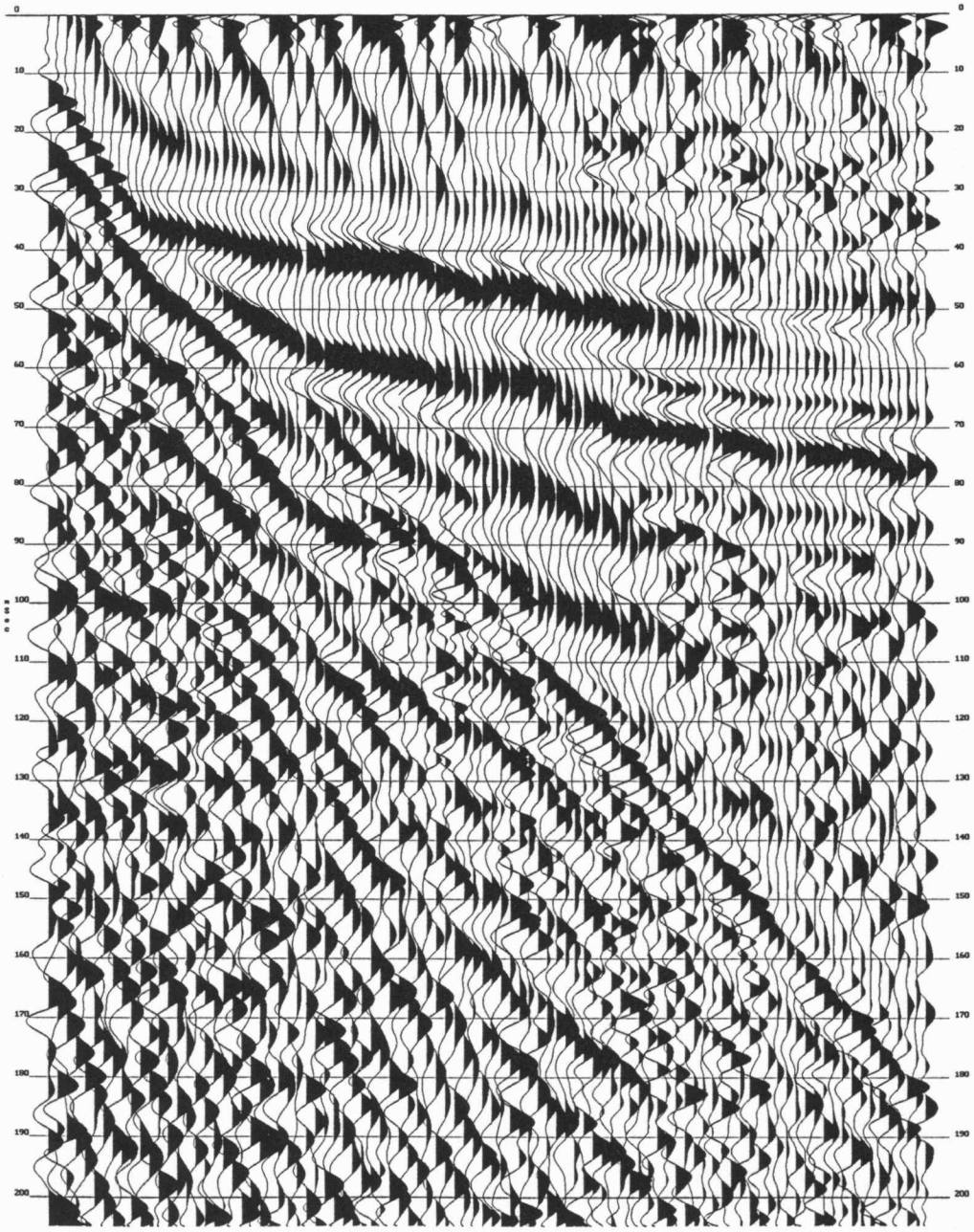
0
10
20
30
40
50
60
70
80
90
100
110
120
130
140
150
160
170
180
190
200

Figure 13c

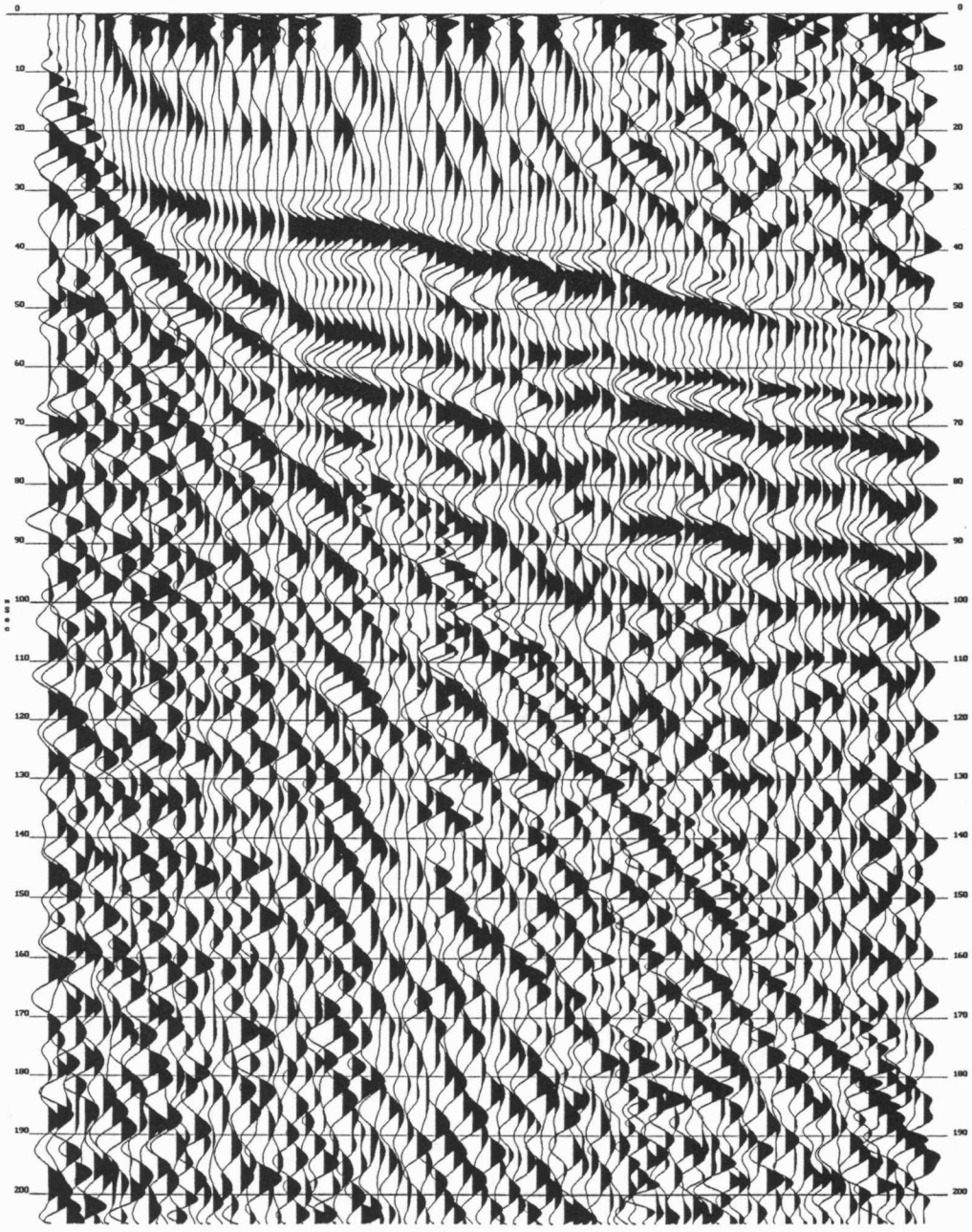
0
10
20
30
40
50
60
70
80
90
100
110
120
130
140
150
160
170
180
190
200
msec

Figure 13d

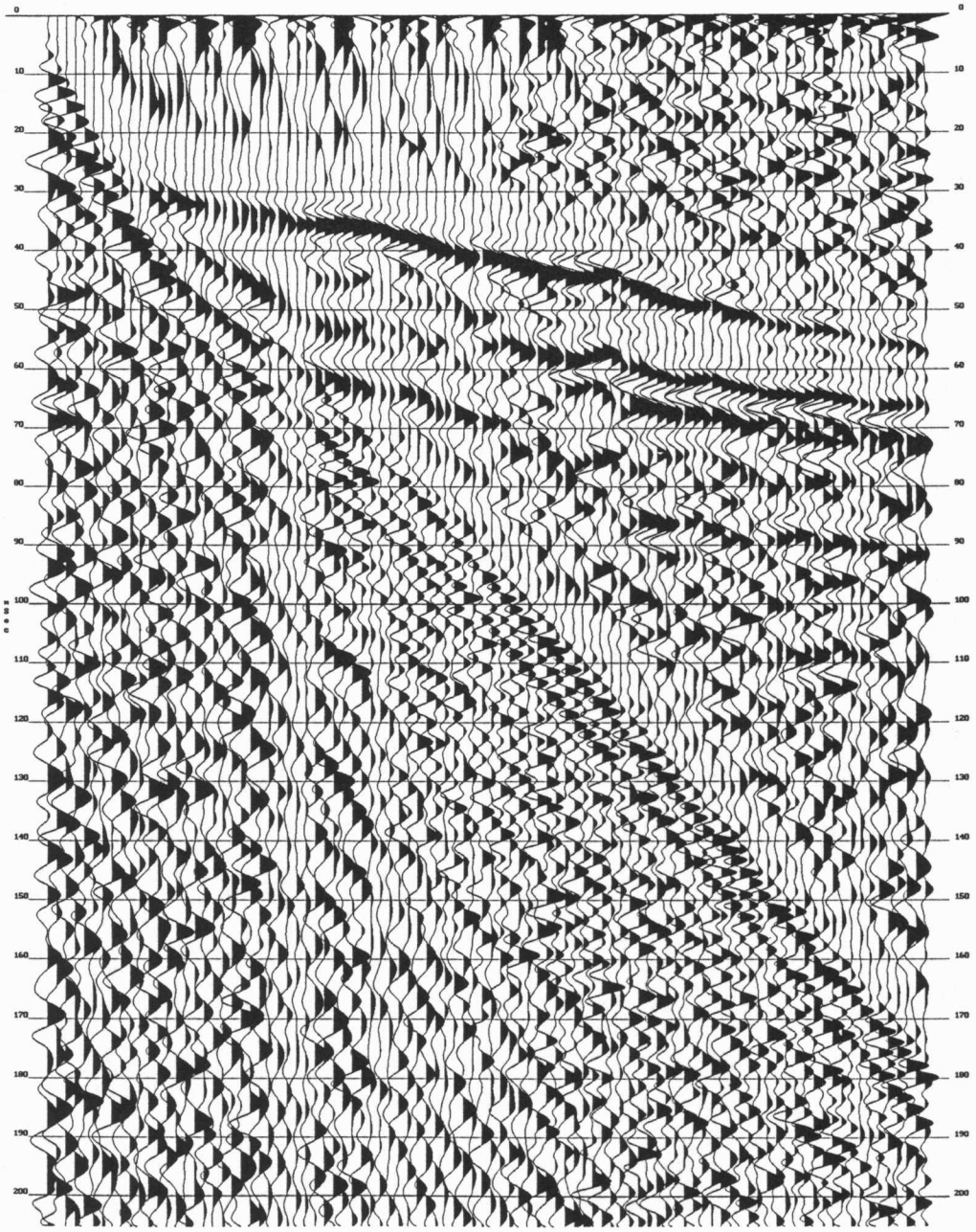
0
10
20
30
40
50
60
70
80
90
100
110
120
130
140
150
160
170
180
190
200

Figure 14

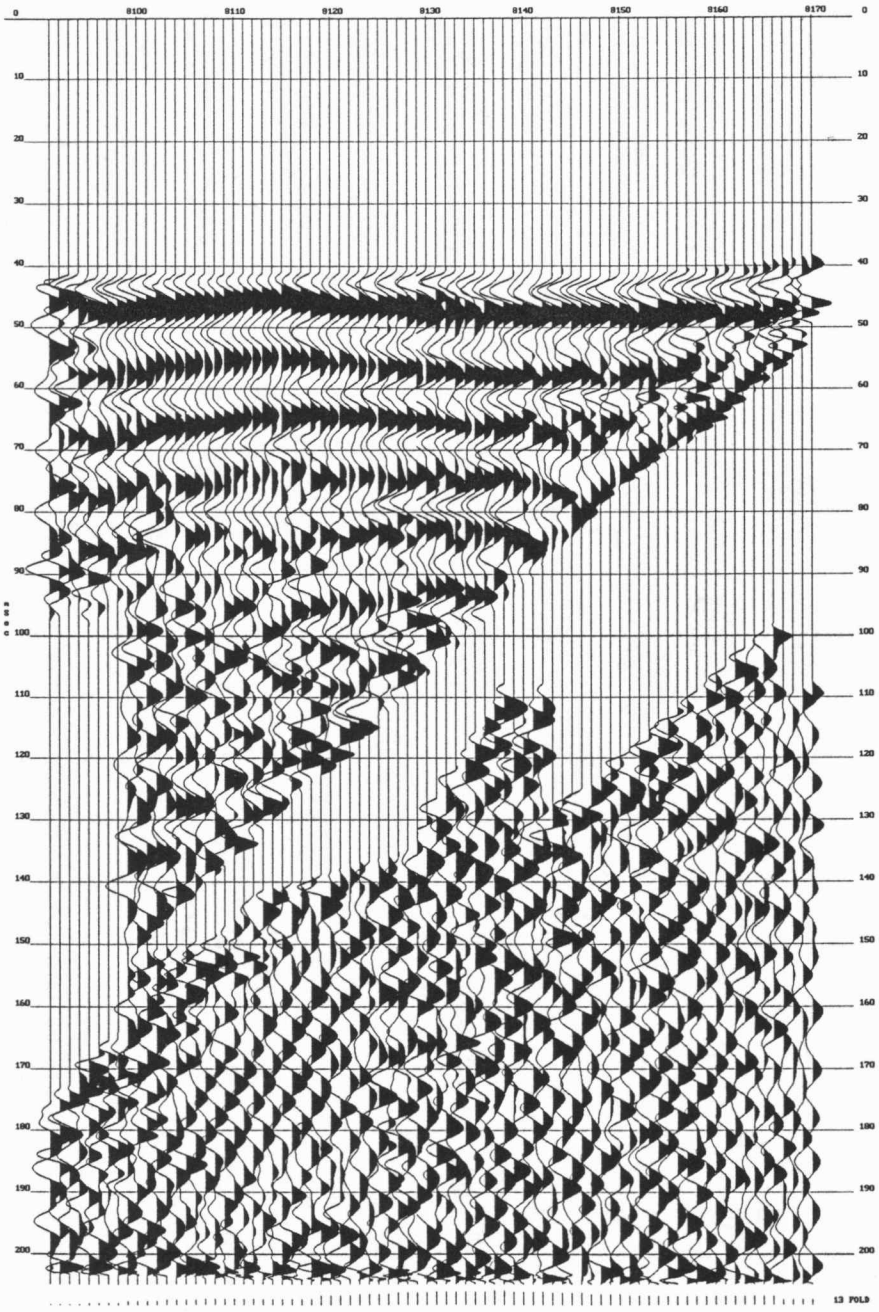
0
8100
8110
8120
8130
8140
8150
8160
8170
0
10
20
30
40
50
60
70
80
90
100
110
120
130
140
150
160
170
180
190
200
msec
13 FOLD

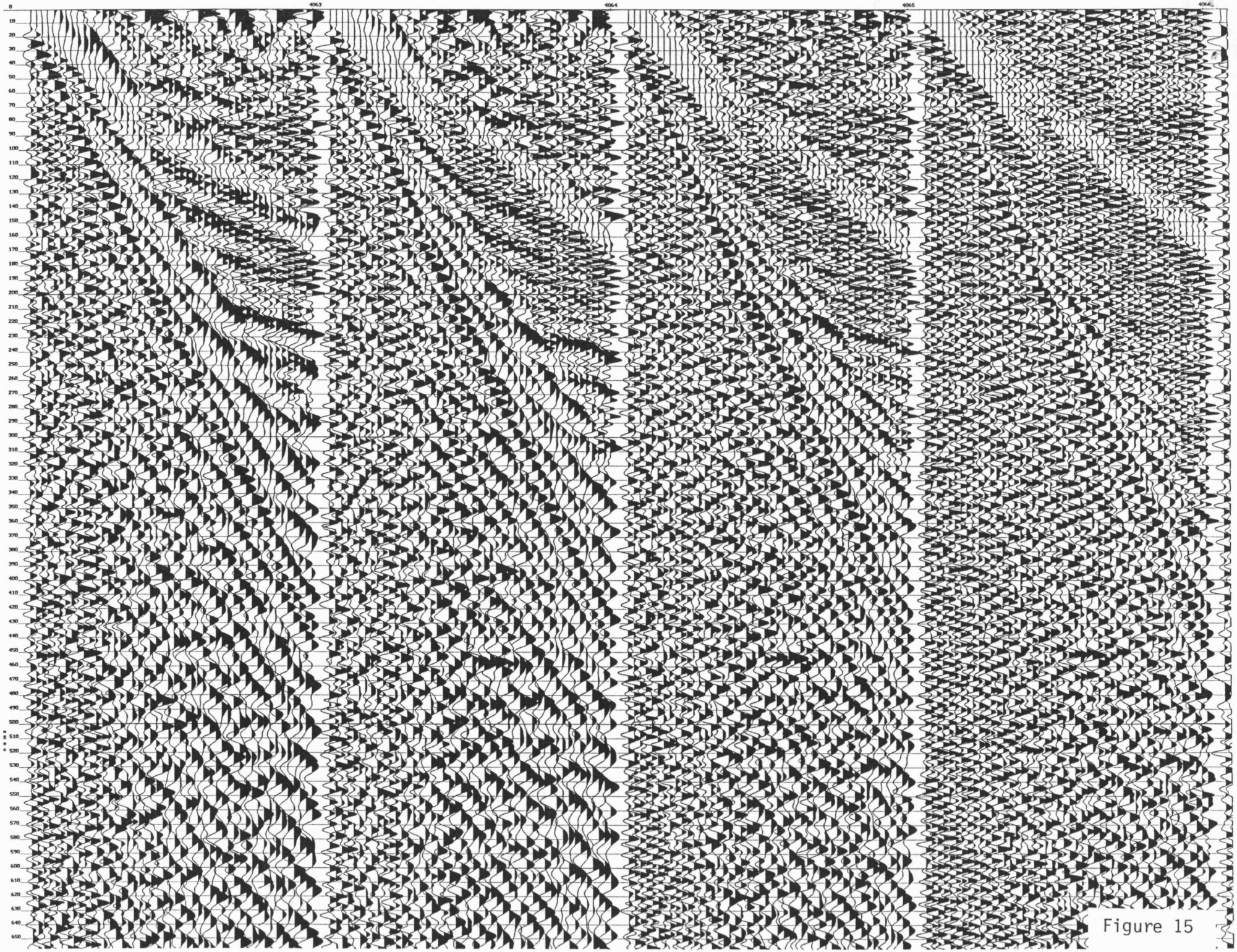

Figure 15